OBSERVATIONS OF INTERSTELLAR MOLECULAR HYDROGEN EMISSION

Thesis by

Steven Van Walter Beckwith

In Partial Fulfillment of the Requirements

for the Degree of

Doctor of Philosophy

California Institute of Technology

Pasadena, California

1978

(Submitted May 25, 1978)

ACKNOWLEDGEMENTS

Most of the work presented in this thesis was done in collaboration with other people. I am particularly grateful to S. E. Persson, I. Gatley, G. Neugebauer, E. E. Becklin, M. Werner, and K. Matthews for the time, effort, and friendship which they gave freely over the last several years.

Two people, N. J. Evans II and S. E. Persson, gave me special support and guidance throughout my years at Caltech. It is my pleasure to thank them for the excellent examples they set as my friends and collaborators.

I am especially grateful to Harriet Holtzman for her love and encouragement during all phases of this work. She provided me with much of the motivation for this thesis.

G. Neugebauer, E. E. Becklin, and M. Werner patiently supervised the research for my experiments. I thank S. Hage, J. Boyer, and G. Forrester for their help with much of the work. This project would not have been possible without the efforts of K. Matthews. He provided both the InSb detector system referred to in the text and excellent advice on many aspects of the experiments.

Many useful discussions were provided by J. Elias, S. Slutz, A. Sargent, W. L. W. Sargent, P. Goldreich, G. Münch, T. Phillips, J. Black, J. Kwan, J. Houck, F. Cordova, R. Blandford, R. Walker, and P. Wannier. I received excellent help with the observations from G. Hancock, H. Lanning, G. Tuton, and J. Carrasco.

I received financial support from Graduate Research Assistantships and, in many times of need, my parents. Support for the experiments came from National Aeronautics and Space Administration grant NGL 05-002-207 and National Science Foundation grant AST74-18555A2.

Finally, I thank my family for their love and devotion which continually reminded me that it was all worthwhile.

ABSTRACT

A search for interstellar molecular hydrogen emission, as seen in the v = 1 → 0 S(1) line, is presented. Thirty-six objects were observed as part of this search; seven objects show emission from vibrationally excited H_2. Of the seven new sources, six are associated with planetary nebulae and one is associated with T Tauri. By considering the current theories of H_2 excitation and comparing the emission line intensities from the new sources with the upper limits to emission from nine HII regions, it is concluded that excitation of the molecules originates in the boundary layers of strong shock waves. The new sources provide a basis for futher study of interstellar H_2 emission, planetary nebulae, and T Tauri stars.

In addition to the search, an in-depth study of the molecular hydrogen emission from the Orion nebula is presented. The data consist of maps at both 13" and 5" resolution in the v = 1 → 0 S(1) emission line. Intensity measurements of the v = 1 → 0 S(0), S(1), S(2), and Q(3) transitions and the v = 2 → 1 S(1) transition are used to derive a vibrational temperature of 2000 K ± 300 K and the associated column densities at the two emission peaks. The data presented here improve upon previous data of the Orion H_2 emission.

Measurements of the v = 1 → 0 Q(3)/S(1) intensity ratio are given. Comparison of this ratio with that observed in NGC 7027 leads to a 2.1 μm extinction of 4.5 magnitudes to the emission region in Orion. A measurement of the Q(4)/S(2) intensity ratio gives a similar value. The extinction implies that the emission region is inside the molecular cloud and probably

near the BN/KL infrared cluster. The extinction measurement is used with previous line intensity measurements to correct the derived excitation temperatures. The resultant rotational and vibrational temperatures of H_2 are found to be equal within the uncertainties.

The measurements of Orion strongly imply that the vibrationally excited molecular hydrogen exists behind the discontinuity of a strong shock wave. A rough estimate of the energy involved in the shock indicates that no observed object in Orion could drive the shock. The results lend support to the suggestion that a supernova explosion occurred within the molecular cloud several thousand years ago.

TABLE OF CONTENTS

INTRODUCTION

The matter in the universe is almost all in the form of hydrogen. Stars are composed of atomic and ionized hydrogen; hydrogen is the fuel for the nuclear reactions which produce starlight. The space between the stars is filled with gas, much of which has condensed into giant clouds. These clouds cool and collapse and eventually they compress the gas to form new stars. Hydrogen, in its molecular form, makes up most of the mass of the clouds and it provides the raw material for star formation. Molecular hydrogen plays a major role in the dynamics of the interstellar medium and the creation of new stars.

In spite of its importance, molecular hydrogen was not observed directly until the last decade. Unlike atomic hydrogen, H_2 has no strong optical or radio wavelength transitions and all of its lines occur at ultraviolet and infrared wavelengths. Observations at these wavelengths are difficult to make. Most of the information we have about H_2 has not come from direct observations of the molecule. We are changing this situation by improving the observational techniques at infrared and ultraviolet wavelengths and observing H_2 in a number of different ways. In particular, new observations of the infrared transitions have identified a number of sources of strong H_2 emission; these sources will be used to test new observational techniques and increase further the available ways of studying the molecule.

Interstellar molecular hydrogen was first observed through its electronic absorption bands at ultraviolet wavelengths. These observations are limited to relatively low density regions seen in projection against nearby, hot stars. It is not possible to study the H_2 in dense molecular clouds using this technique. Because the earth's atmosphere is opaque at the wavelengths of the bands, the measurements must be made from rockets and satellites. The cost and lack of flexibility of the observations are a great disadvantage for any scientific study of H_2.

In addition to electronic energy levels, molecular hydrogen has a number of lower energy vibrational and rotational states. Most of the transitions between these states emit radiation at infrared wavelengths. These transitions can be observed using ground based telescopes. The ease and comparatively low cost of such observations are a great advantage over those of the ultraviolet absorption bands. Infrared spectroscopy has recently become sensitive enough to make a study of interstellar H_2 practical. The transition probabilities between the relevant states are very small, typically of order 10^{-7} s^{-1}. The infrared emission lines have relatively small intensities and require sensitive infrared detection techniques. It was not until 1976 that the infrared emission spectrum of interstellar H_2 was observed.

Recent advances in infrared detector technology have made these observations substantially more practical. The advances have been particularly important for infrared spectroscopy since the limiting noise of short wavelength infrared spectrometer systems is detector noise. The development of InSb detectors for use at infrared wavelengths has considerably decreased the detector noise. It is this advance in technology that has made a study of H_2 emission possible.

In this thesis, observations of infrared emission from interstellar molecular hydrogen are presented. The instrument used to make the observations is a grating spectrometer of moderate spectral resolution ($\Delta\lambda/\lambda \simeq 10^{-3}$). The spectrometer itself was built over ten years ago for rocket experiments. It was modified for use on ground based telescopes by D. McCammon, G. Münch, and G. Neugebauer over ten years ago. These scientists laid the groundwork for the current experiment. Additional modifications have been made for this experiment and the spectrometer has been interfaced with an InSb detector system. This system is one of the most sensitive that is currently available for work at wavelengths near those of the observed H_2 lines.

Even so, the sensitivity is barely adequate for the study presented here.

The thesis consists of a table and four papers. The table and first two papers give the results of a search for molecular hydrogen from a variety of celestial objects. The papers were written in collaboration with I. Gatley, K. Matthews, G. Neugebauer, and S. E. Persson and published in the Astrophysical Journal. These papers describe the discovery of six sources of molecular hydrogen emission. The table lists all of the objects surveyed for H_2 emission. Of the nine currently known sources of H_2 emission, six were found in this survey. The discovery of new sources of emission is essential to future studies of molecular hydrogen.

Papers 3 and 4 describe the results of an in-depth study of H_2 emission from the Orion nebula. This is the most complete study of the Orion emission to date. These papers were written in collaboration with E. E. Becklin, G. Neugebauer, and S. E. Persson and submitted for publication to the Astrophysical Journal. Paper 3 presents observations which show the location and extent of the emission. The results of this paper, when combined with the results of Paper 4, give the temperature and column density of the observed molecules. Paper 4 presents observations which give the extinction to the emission region in Orion. Knowledge of the extinction allows a derivation of the actual surface brightness and luminosity from the observations. With these quantities, the energetics of the emission can be studied.

A brief discussion of the results of these papers is given at the end of the thesis. The results of the survey are summarized in the first section and a discussion of Orion is presented in the second. The results of Papers 3 and 4 are used together to give an overview of Orion. The discussion summarizes major results and conclusions regarding the physical conditions within the emission region. It also includes a brief discussion of the nature of the source.

RESULTS OF THE SEARCH FOR H_2 EMISSION

OBJECT	TYPE[a]	DATE	TELESCOPE[b]	METHOD[c]	APERTURE[d] (arc-sec)	SPACING[e] (arc-sec)	RESOLUTION (Å)	DISTANCE[f] (kpc)	R.A. (1950)	DEC. (1950)	AREA[g] SEARCHED	$v = 1 \rightarrow 0$ S(1)[h] INTENSITY (10^{-4} erg s^{-1} cm^{-2} sr^{-1})	SIZE (arc-sec)	LUMINOSITY[i]	NOTES
NGC 40	PN	77 Jul 19	24	B	36	216 EW	17	1.8	$00^h10^m16.5^s$	+72°14'39"	α,δ	< 2.4	40		
NGC 650-1	PN	77 Sep 8	24	B	36	216 EW	17	0.8	01 39 09.6	+51 19 02	α,δ	1.8±1.2	90		
											α,δ±54"	1.8			
VV 8	PN	77 Sep 24	100	B	10	60 NS	17	< 3	01 55 32.9	+52 39 15	α,δ	1.0	< 0.5		
CRL 618	PN	77 Aug 24	100	B	10	60 NS	17	< 5	04 39 33.8	+36 01 15	α,δ	2.6±0.4	< 5	< 0.4	
		78 Mar 24	200	B	5	30 NS	17				α,δ	12±1			
IC 418	PN	76 Dec 9	100	F	10	---	17	1.8	05 25 09	-12 44 12	α,δ	1.7±1.1	12		
NGC 2440	PN	77 Dec 18	100	B	15	60 NS	26	1.4	07 39 41.5	-18 05 28	α,δ	0.6±0.1	15	0.02	4
NGC 6543	PN	77 Jul 19	24	B	36	216 EW	17	1.1	18 02 21	+23 22 00	α,δ	< 1.9	20		
NGC 6572	PN	77 Aug 14	100	B	10	60 NS	17	1.7	18 09 40.6	+06 50 26	α,δ	< 1.2	10		
NGC 6720	PN	77 Aug 28	100	B	20x10	90 NS	300	1.3	18 51 43.0	+32 58 20	α,δ	1.4±0.1	60	0.02	7
NGC 6790	PN	77 Aug 15	100	B	10	60 NS	17	0.5	19 20 24.9	+01 25 01	α,δ	< 1.0	9		
BD +30°3639	PN	77 Aug 3	100	B	10	60 NS	17	8	19 32 47.6	+30 24 17	α,δ	1.9±0.5	3	0.7	
V1016 CYG	PN	77 Jun 7	100	F	10	---	19	3	19 55 18.0	+39 41 24	α,δ	< 1.3			
IC 4997	PN	77 Aug 15	100	B	10	60 NS	17	8.6	20 17 53	+16 34 27	α,δ	0.5±0.2	1		
CRL 2688	PN	77 Sep 21	100	B	10	60 NS	17		21 00 19.9	+36 29 45	α,δ	2.0±0.4	10		8
NGC 7009	PN	77 Sep 8	24	B	36	216 EW	17	1.2	21 01 27.5	-11 33 42	α,δ	1.2±0.9	14		
											α±31",δ	< 2.5			
NGC 7027	PN	76 Dec 8	100	B	10	60 NS	17	1	21 05 09.4	+42 02 03	α,δ	6±1	8	0.03	
Hb 12	PN	77 Aug 14	100	B	10	60 NS	17		23 23 57.2	+57 54 24	α,δ	1.6±0.3	< 1		9
RY Tau	TT	77 Oct 3	200	B	5	30 EW	17	0.15	04 18 51.0	+28 19 29	α,δ	< 3	< 5		
T Tau	TT	77 Sep 24	100	B	10	60 NS	17	0.15	04 19 04.4	+19 24 59	α,δ	3.5±0.5	5	0.0005	
		77 Oct 3	200	B	5	30 EW	17				α,δ	6.2±1.0			
HL Tau	TT	77 Oct 3	200	B	5	30 EW	17	0.15	04 24 44.5	+18 07 32	α,δ	< 4	< 5		
DK Tau	TT	77 Oct 3	200	B	5	30 EW	17	0.15	04 27 40.7	+25 54 53	α,δ	< 3	< 5		
SU Aur	TT	77 Oct 3	200	B	5	30 EW	17	0.15	04 52 47.9	+30 29 14	α,δ	< 3	< 5		
W3 IRS1	HII	76 Oct 18	60	B	13	96 NS	30	3	02 21 56.0	+61 52 45	α,δ	1.0±0.5	30		
θ^2 Ori	HII	76 Oct 24	100	B	13	60 NS	19	0.5	05 32 54.0	-05 26 51	α,δ	1.1±0.4	20		2
		77 Sep 21	100	B	10	60 NS	17		05 32 53.8	-05 26 51	α,δ	0.4±0.4			3
NGC 2023	HII	78 Mar 16	24	B	54	216 EW	38	0.4	05 39 07	-02 16 58	α,δ	1.0±0.4	> 100		
Mon R2 IRS1	HII	76 Nov 29	60	B	16	96 NS	17	1	06 05 20.0	-06 22 33	B	< 2.5	50		
S 255	HII/MC	76 Dec 10	100	T	10	---	21	1	06 09 58.4	+18 00 11	D	< 30	> 200		
M17	HII/MC	77 Jun 15	24	F	36	---	17	2.4	18 17 26.5	-16 14 54	E	< 6.0	600		
		77 Jul 11	24	F	36	216 EW	17				F	< 7.1			
K3-50A	HII/MC	76 Oct 25	100	B	13	60 NS	20	8	19 59 50.1	+33 24 19	α,δ	0.5±0.3	10		
S106	HII	77 Sep 24	100	B	10	60 NS	17	2	20 25 33.8	+37 12 52	H	< 4.3	60		
NG 7538 IRS2	HII/MC	76 Dec 7	100	B	10	60 NS	17	3.5	23 11 37.0	+61 11 57	α,δ	< 1.0	10		
W3 IRS5	MC/IR	76 Dec 8	100	B	10	60 NS	17	3	02 21 53.2	+61 52 21	α,δ	< 1.1	< 1		
W3	MC	76 Dec 9	100	F	10	60 NS	17		02 21 56.8	+61 52 42	A	< 6.9	60		
Orion Pk1	MC	76 Nov 5	200	F	5	30 NS	17	0.5	05 32 46.2	-05 24 01	α,δ	90±5	80	2.5(150)	1
		76 Oct 24	100	B	10	60 NS	17					65±5			
Mon R2 IRS3	MC/IR	76 Nov 29	60	B	16	96 NS	17	1	06 05 21.8	-06 22 26	α,δ	1.5±0.5	< 1		
		76 Dec 6	100	T	10	---	17				α,δ	1.5±1.4	< 1		
		76 Dec 10	100	T	10	---	21				C	< 15	60		
S 140	MC	77 Jun 15	24	F	36	---	17	0.9	22 17 41.3	+63 03 49	α,δ	< 3.9	240		
IRC +10216	IR	76 Dec 7	100	B	10	60 NS	17	0.3	09 45 14.8	+13 30 41	α,δ	< 30	< 1		5
Ophiuchus VS1	IR	77 Jun 7	100	F	10	---	19	0.2	16 23 16.7	-24 21 29	α,δ	< 2.3	< 1		
											α,δ±10"	< 3.8			
Sgr A	IR	77 Jun 7	100	F	10	---	19	10	17 42 29.8	-28 59 20	α,δ	< 3.9	> 100		
M 82	G	76 Nov 29	60	B	16	96 NS	17	3200	09 51 43.6	+69 55 05	Nucleus	0.6±0.2	15		6
		76 Dec 2	200	F	5	30 NS	17				Nucleus	< 0.9			
W 44	SNR	77 Sep 14	24	B	36	216 EW	17	3	18 54 34	+01 15 36	G	< 2.8	600		

SUPERSCRIPT NOTES

(a) PN - planetary nebula, H II - H II region, MC - molecular cloud, IR - infrared continuum source, TT - T Tauri star, G - galaxy, SNR - supernova remnant. Some sources do not strictly belong to the categories under which they are classified.

(b) 24 - Mount Wilson 24-inch, 60 - Mount Wilson 60-inch, 100 - Hooker 100-inch, 200 - Hale 200-inch.

(c) B - beam switching for sky subtraction,
F - frequency switching,
T - two detectors measure line and continuum wavelengths simultaneously (see Paper 3).

(d) Circular apertures except for NGC 6720 which is rectangular (α x δ).

(e) Dash indicates use of reference blackbody at ambient temperature (see Paper 3).

(f) Distances are given when known. These distances are not all known accurately.

(g) α,δ refers to the position given in the table. When a letter reference is given, detailed position information is given in the notes.

(h) All results larger than 1σ are given. All upper limits are 3σ. A measurement was not considered to be a detection of H_2 emission unless at least two separate 3σ results were obtained.

(i) Luminosity of the $v = 1 \rightarrow 0$ S(1) transition.

NOTES TO THE TABLE

1. Luminosity obtained by integration of surface brightness map given in Paper 3. Number in parenthesis is luminosity after correction for extinction.

2. Search position is 21" West of θ^2 Ori.

3. Search position is 24" West of θ^2 Ori.

4. Measured twice, both measurements were 4σ detections.

5. Limit is 3% of continuum intensity.

6. Measured only once, not considered a confirmed detection. Redshift of 186 km s^{-1} used for line center.

7. Luminosity computed by assuming an average surface brightness of 6×10^{-5} ergs s^{-1} cm^{-2} sr^{-1} over the solid angle of the ring of 1.5×10^{-8} sr.

8. Distance not known.

9. Distance not known.

AREA SEARCHED NOTES

A Offsets from the position of IRS 2 :

(10" N; 20" W, 10" W, 0" E, 10" E, 20" E)

(10" S; 0" E)

(20" S; 0" E, 10" W, 20" W, 30" W)

(18" S; 35" W)

IRS 4

B Offsets from (α ; δ) :

(5" N; 0" E)

(5" S; 0" E, 10" W)

(10" S; 0" E)

C Offsets from (α ; δ) which is the position of IRS 3 :

(20" N; 0" E)

(10" N; 0" E)

(0" N; 50" W, 40" W, 30" W, 20" W, 10" W, 0" E, 10" E, 20" E, 30" E)

(10" S; 0" E)

(20" S; 0" E)

(30" S, 0" E)

D Offsets from (α ; δ) which is the position of the infrared source :

(0" N; 50" W, 40" W, 30" W, 20" W, 10" W, 0" E, 10" E, 20" E, 30" E,
40" E, 50" E)

E Offsets from (α ; δ) :

(180" N; 0" E, 36" E, 72" E, 108" E, 144" E, 180" E)

(144" N; 0" E)

(108" N; 0" E)

(72" N; 0" E)

(36" N; 36" W, 0" E, 36" E, 72" E)

(0" N; 36" W, 0" E, 36" E, 72" E)

(36" S; 36" W, 0" E, 36" E, 72" E)

F Offsets from (α ; δ) as in E above:

(704" N; 169" E) - northern CO peak

(36" N; 36" E)

(0" N; 0" E, 36" E)

(36" S; 36" E)

(72" S; 36" E, 72" E)

(108" S; 36" E, 72" E)

(144" S; 36" E, 72" E)

(180" S; 36" E)

G Offsets are from (α ; δ) which is the position of most intense CO emission :

(0" N; 360" W, 288" W, 216" W, 144" W, 72" W, 0" E, 72" E, 144" E, 216" E, 288" E, 360" E)

H Offsets from (α : δ) which is the position of the infrared source :

(0" N; 10" W, 0" E, 10" E, 20" E, 30" E)

(9" S; 4" E)

(19" S; 4" E)

PAPER 1:

DETECTION OF MOLECULAR HYDROGEN EMISSION FROM FIVE PLANETARY NEBULAE

Published in the Astrophysical Journal,

Volume 219, page L33, in

collaboration with

S. E. Persson and I. Gatley

I. INTRODUCTION

Emission from molecular hydrogen was first discovered in the Orion Nebula by Gautier et al. (1976) and subsequently in NGC 7027 by Treffers et al. (1976). We have searched for the $v = 1 \rightarrow 0$ S(1) line of H_2 in nine planetary nebulae and their supposed progenitors (Zuckerman et al. 1976; Humphreys, Warner and Gallagher 1976); positive detections were achieved in five of these; namely, the Ring Nebula (M57; NGC 6720), BD+30°3639, Hb 12 (Perek and Kohoutek 1967, No. 111 - 2°1), CRL 618 (Westbrook et al. 1975), and CRL 2688 (Ney et al. 1975; Price and Walker 1976).

All of the objects with detectable H_2 emission are known to emit the λλ6300 or 6363 lines of [OI]. These lines are excited in transition zones between neutral and ionized hydrogen, and can indicate the presence of high density neutral clumps within the ionized region (Capriotti, Cromwell and Williams 1971; Van Blerkom and Arny 1972; Capriotti 1973; Goad 1975; Cohen and Kuhi 1977). In the case of the Ring Nebula it is shown that the molecular hydrogen emission is spatially correlated with the [OI]. In this letter we present the observational results and only a brief discussion. More detailed analysis will be given in a later paper (Beckwith et al. 1978b).

II. OBSERVATIONS

The observations reported in this Letter were made on the 2.5 m Hooker telescope and the 0.6 m telescope on Mt. Wilson during 1977 August. Two spectrometers were used: a grating spectrometer with 17 Å (3.8 cm^{-1}) resolution and a circular variable filter wheel (CVF) with resolution

$\Delta\lambda/\lambda = 0.014$. The grating spectrometer system and observing procedure are described in detail by Beckwith et al. (1978a); for the present observations a circular aperture 10" in diameter with a 60" beam spacing for sky subtraction was used. No airmass correction has been applied to data taken with this spectrometer. The CVF system is described in detail by Neugebauer et al. (1976); for the present observations a 20" x 10" (α x δ) aperture was used with a 90" beam spacing for sky subtraction. The airmass correction given by Neugebauer et al. (1976) has been applied to data taken with the CVF.

Flux calibration was achieved by observing α Lyr, α Cyg and 4 Lac, whose 2.2 μm magnitudes are 0.00, 0.90, and 4.25 respectively. Each standard is assumed to have a Rayleigh-Jeans continuum in the 2 μm atmospheric window.

The map of the northeast quadrant of the Ring Nebula was made with the CVF by sampling at points separated by 20" in right ascension and 10" in declination. The map covers a region 80" in right ascension by 50" in declination and is shown in Figure 1. At each location four wavelengths were measured: 2.122 μm ($v = 1 \rightarrow 0$ S(1)), 2.166 μm (Brackett γ), 2.081 μm and 2.209 μm (continuum). There could be some contamination of the 2.081 μm point by the 2.06 μm line of He I; its effect has been ignored. In addition to the map a declination scan over the northern part of the ring was made by sampling every 5" along a line 5" west of the central star of the nebula. In both the map and the scan the relative spatial uncertainty between the Brackett γ and H_2 measurements is no more than 2".

A complete CVF spectrum of the brightest point in the Ring Nebula was obtained on the 0.6 m telescope on Mt. Wilson. A similar spectrum of CRL 2688 was obtained on the 2.5 m Hooker telescope and is shown in Figure 4.

III. RESULTS

Table 1 lists the strengths of the $v = 1 \rightarrow 0$ S(1) line of H_2, and the Brackett γ line for the five nebulae in which H_2 emission was detected, and lists the $(3\sigma_m)$ upper limits to the S(1) line strengths for the four nebulae not detected in molecular hydrogen. The identification as molecular hydrogen emission was confirmed by complete CVF spectra of CRL 2688 and the brightest point in the Ring Nebula. Both spectra clearly show the $v = 1 \rightarrow 0$ S(1) and S(0) lines and the spectrally unresolved Q branch lines (see Figure 4).

a) The Ring Nebula

Figure 1 shows surface brightness maps of H_2 and Brackett γ emission superposed on a red photograph of the nebula. The surface brightness of both species of emission, like the optical continuum, are in the shape of a ring. The striking difference between the Brackett γ and H_2 maps is that the molecular emission lies outside the atomic emission. This result is emphasized in Figure 2a, which shows the declination scan along the line 5" west of the central star. The peak brightness of the molecular hydrogen lies approximately 5" outside the peak brightness of the atomic hydrogen.

For comparison, Figure 2b shows corresponding scans in the light of Hβ (λ4861) and [OI] (λ6300); these scans have been synthesized from the data of Goad (1975) to have the same spatial resolution as the infrared scans of Figure 2a. For the purposes of presentation the peak of the Hβ scan has been normalized to the peak intensity of Brackett γ, and the [OI] to the intensity of S(1). There is extremely close correspondence in the distribution of surface brightness between the Hβ and Brackett γ, and between the [OI] and molecular hydrogen emission. This correlation also holds for the rest of the region mapped.

b) BD+30°3639, Hb 12, CRL 618

Figure 3 shows the measured profile of the $v = 1 \rightarrow 0$ S(1) line in the objects BD+30°3639, Hb 12 and CRL 618. The dashed line shows the continuum level established from the extreme points of each spectrum (i.e., outside the expected S(1) profile); in each case this continuum level is consistent with a 2.2 μm broadband measurement. Although the signal-to-noise ratio is rather low, there is some indication that the S(1) line in CRL 618 is blueshifted by 4 Å, corresponding to $v_{LSR} \sim$ -35 km/sec. This is consistent to within the measurement uncertainties with the velocity $v_{LSR} \sim$ -50 km/sec found by Westbrook et al. (1975).

c) CRL 2688

Figure 4 shows the CVF spectrum of CRL 2688. The molecular hydrogen emission lines $v = 1 \rightarrow 0$ S(1), S(0), and the Q branch are clearly seen in this spectrum. At the resolution of the CVF it is difficult to fit a continuum level to the observations. The Brackett γ line is not

positively detected; this emphasizes that the strength of molecular hydrogen emission is not correlated with the strength of Brackett γ emission.

IV. DISCUSSION

The principal result of this Letter is that H_2 molecules are found in planetary nebulae. The detectable objects span a wide range in age and morphology: CRL 618 and CRL 2688 are thought to be progenitors of planetary nebulae (Westbrook et al. 1975; Ney et al. 1975; but see also Humphreys, Warner and Gallagher 1976), NGC 7027, BD+30°3639, and Hb 12 are young, high density ($NE_e \geq 10^4$ cm^{-3}) nebulae (Kaler 1970, O'Dell 1963) and NGC 6720 is an old nebula in which the electron density in the diffuse regions is only ~ 600 cm^{-3} (Aller, Epps and Czyzak 1976). The difference in age between these objects is at least a few thousand years. The detection of H_2 in CRL 618 and CRL 2688 may provide support for the suggestion that these objects are, in fact, destined to become classical planetary nebulae.

The second result of this Letter is that the H_2 and [OI] emission line strengths are spatially correlated in NGC 6720. The nature of this correlation cannot be derived in detail from the present data but the overall similarity of the declination scans of H_2 and [OI] in Figure 2 shows that it is likely that the molecules are intimately associated with the [OI] clumps visible on interference filter photographs (Capriotti, Cromwell and Williams 1971; Goad 1975). A comparison of the line ratios $v = 1 \rightarrow 0$ S(1)/Brackett γ and [OI]/Hβ from object to object tends to show a similar correlation. In view of the fact that

the [OI] emission must arise in the transition zones (ionized to neutral) or in the shadows of dense filaments optically thick to the Lyman continuum radiation (Van Blerkom and Arny 1972), it is plausible, as predicted by Capriotti (1973), that the H_2 molecules reside inside the clumps, protected from the dissociating radiation by dust grains.

NGC 7027, BD+30°3639 and the Ring Nebula have been searched for CO emission (Mufson, Lyon and Marionni 1975). The data show that a molecular cloud surrounds the optical nebula NGC 7027. In BD+30°3639 and the Ring Nebula CO was not detected at a level more than an order of magnitude less than that from NGC 7027. The present H_2 results are very different: the strength of the H_2 $v = 1 \rightarrow 0$ S(1) line in NGC 7027 is only three times brighter than that in BD+30°3639. It thus appears that a molecular cloud is not necessary for H_2 emission. This supports the hypothesis that the molecular hydrogen exists inside the neutral clumps.

TABLE 1

MEASUREMENTS OF PLANETARY NEBULAE

Object	H_2 (2.122μ) v = 1→0 S(1) line ± 1 σ_m 10^{-13} erg s^{-1} cm^{-2}	HI (2.166μ) Brackett γ line ± 1 σ_m 10^{-13} erg s^{-1} cm^{-2}	Notes
NGC 6720	6.8 ± 0.4	2.1 ± 0.3	2, 3
BD+30°3639	3.5 ± 0.9	66 ± 6	1
Hb 12	3.0 ± 0.5	31 ± 4	1
CRL 618	4.8 ± 0.8	< 4	1, 5
CRL 2688	5 ± 2	2 ± 2	2, 4
NGC 6572	< 2.6	105 ± 10	5
IC 4997	< 2.6	15 ± 2	5
NGC 6790	< 2	14 ± 2	5
V1016 Cyg	< 3.3	---	5

Notes:

1. Measurement made with grating spectrometer
2. Measurement made with CVF system.
3. Brightest point in a 10" x 20" aperture.
4. Large error results from uncertain continuum.
5. Upper limits are 3 σ_m.

REFERENCES

Aller, L. H., Epps, H. W., and Czyzak, S. J. 1976, Ap. J., 205, 798.

Beckwith, S., Persson, S. E., Neugebauer, G., and Becklin, E. E. 1978a, in preparation.

Beckwith, S., Persson, S. E., Gatley, I., and Neugebauer, G. 1978b, in preparation.

Capriotti, E. R., Cromwell, R. H., and Williams, R. E. 1971, Ap. Lett., 7, 241.

Capriotti, E. R. 1973, Ap. J., 179, 495.

Cohen, M. H., and Kuhi, L. V. 1977, Ap. J., 213, 79.

Gautier, T. N. III, Fink, U., Treffers, R. R., and Larson, H. P. 1976, Ap. J. (Letters), 207, L129.

Goad, L. E. 1975, Ph.D. thesis, Harvard University.

Humphreys, R. M., Warner, J. W., and Gallagher, J. S. 1976, PASP, 88, 380.

Kaler, J. B. 1970, Ap. J., 160, 887.

Mufson, S. L., Lyon, J., and Marionni, P. A. 1975, Ap. J. (Letters), 201, L85.

Neugebauer, G., Becklin, E. E., Beckwith, S., Matthews, K., and Wynn-Williams, C. G. 1976, Ap. J. (Letters), 205, L139.

Ney, E. P., Merrill, K. M., Becklin, E. E., Neugebauer, G., and Wynn-Williams, C. G. 1975, Ap. J. (Letters), 198, L129.

O'Dell, C. R. 1963, Ap. J., 138, 293.

Perek, L., and Kohoutek, L. 1967, Catalogue of Galactic Planetary Nebulae (Prague: Academia).

Price, S. D., and Walker, R. G. 1976, Air Force Geophysics Laboratory, No. 576, AFGL-TR-76-0208.

Treffers, R. R., Fink, U., Larson, H. P., and Gautier, T. N. III. 1976, Ap. J., 209, 793.

Van Blerkom, D., and Arny, T. T. 1972, M.N.R.A.S., 156, 91.

Westbrook, W. E., Becklin, E. E., Merrill, K. M., Neugebauer, G., Schmidt, M., Willner, S. P., and Wynn-Williams, C. G. 1975, Ap. J., 202, 407.

Zuckerman, B., Gilra, D. P., Turner, B. E., Morris, M., and Palmer, P. 1976, Ap. J. (Letters), 205, L15.

FIGURE CAPTIONS

Fig. 1 Partial maps of H_2 surface brightness and Brackett γ (Bγ) surface brightness overlayed on a picture of the Ring Nebula taken on the 200 inch Hale telescope through a red filter. The beam size is shown by the cross hatched area on each map. Northeast is in the upper lefthand corner. Labelled contour levels are in units of 10^{-5} ergs s^{-1} cm^{-2} sr^{-1} for both maps. The distance between the central star and the bright star directly east of the nebula is 60".

Fig. 2 Scans taken along a line 5" west of the central star with the abscissa indicating the declination offset north of the central star. The resolution was 10" as indicated by FWHM. Lines are drawn between the points as an aid to the eye. Plot of Hβ and [OI] λ6300 surface brightness derived from the data of Goad (1975). The Hβ profile is normalized so that the peak brightness is the same height as the peak brightness in Brackett γ (Bγ). Similarly, the [OI] peak is normalized to the H_2 peak. The spatial resolution of Goad's original work has been degraded here to match the spatial resolution of the Brackett γ and H_2 observations.

Fig. 3 The measurements of BD+30°3639, Hb 12 and CRL 618 made with the grating spectrometer system. The intensity and wavelength scales are the same for all plots. The continuum flux level was determined by averaging the points that are

18 Å or more from the line center. In each case the measured instrumental profile, appropriately normalized and centered, has been drawn through the data to aid the eye.

Fig. 4 The spectrum of CRL 2688 taken with the CVF. The zero level has been suppressed. The wavelengths of Brackett γ (Bγ) and six molecular hydrogen lines are marked for comparison and the points are connected to aid the eye wherever the sampling was complete.

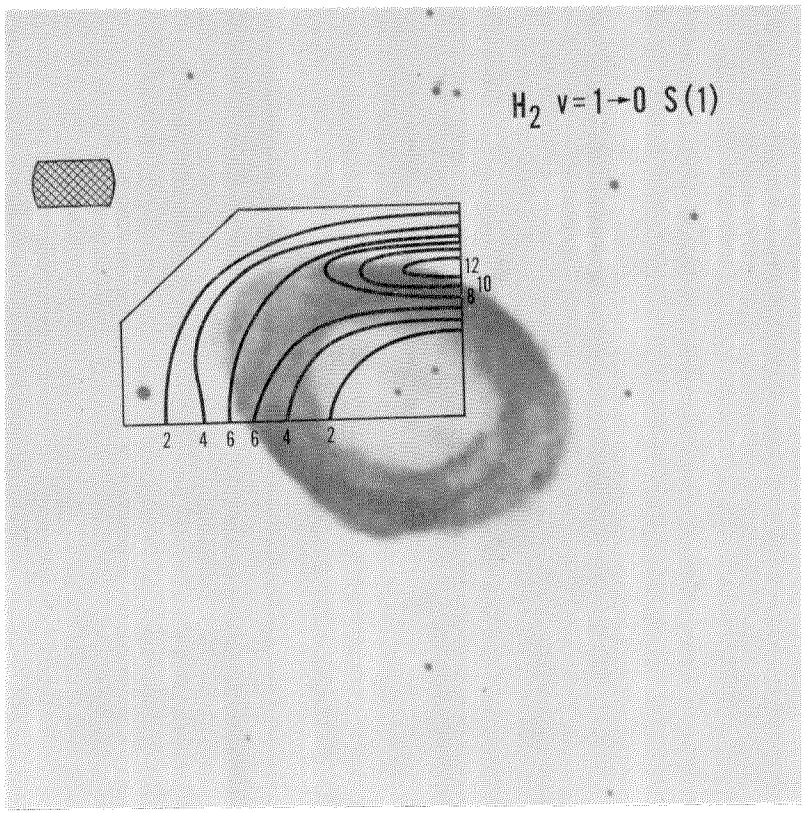

FIG. 1*a*

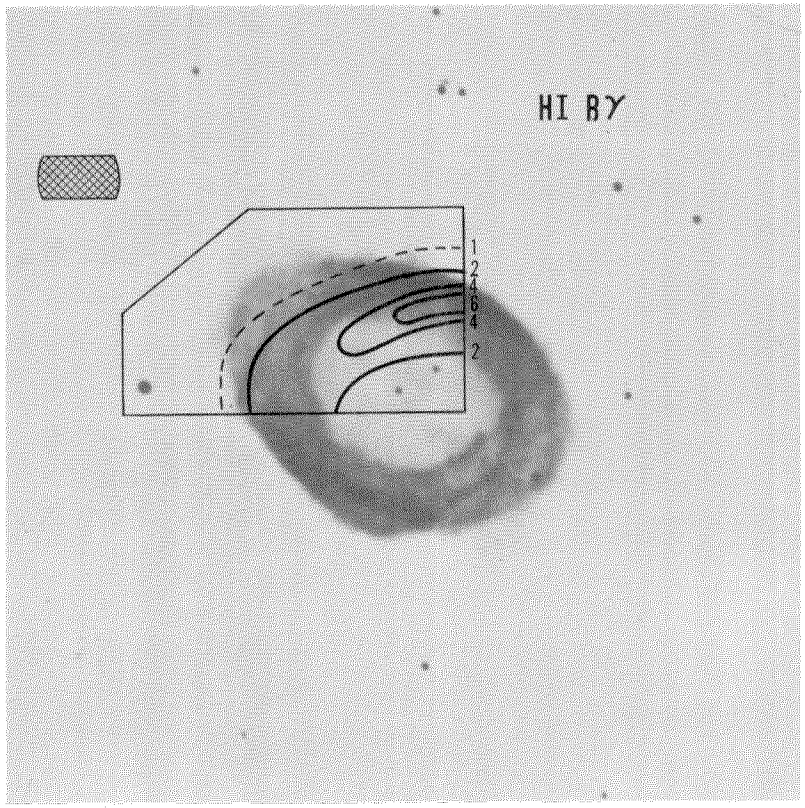

FIG. 1*b*

FIG. 1.—Partial maps of H_2 surface brightness (*a*) and Bγ surface brightness (*b*) overlayed on a picture of the Ring Nebula taken on the 200 inch (5.08 m) Hale telescope through a red filter. The beam size is shown by the crosshatched area on each map. Northeast is in the upper left corner. Labeled contour levels are in units of 10^{-5} ergs s^{-1} cm^{-2} sr^{-1} for both maps. The distance between the central star and the bright star directly east of the nebula is 60″.

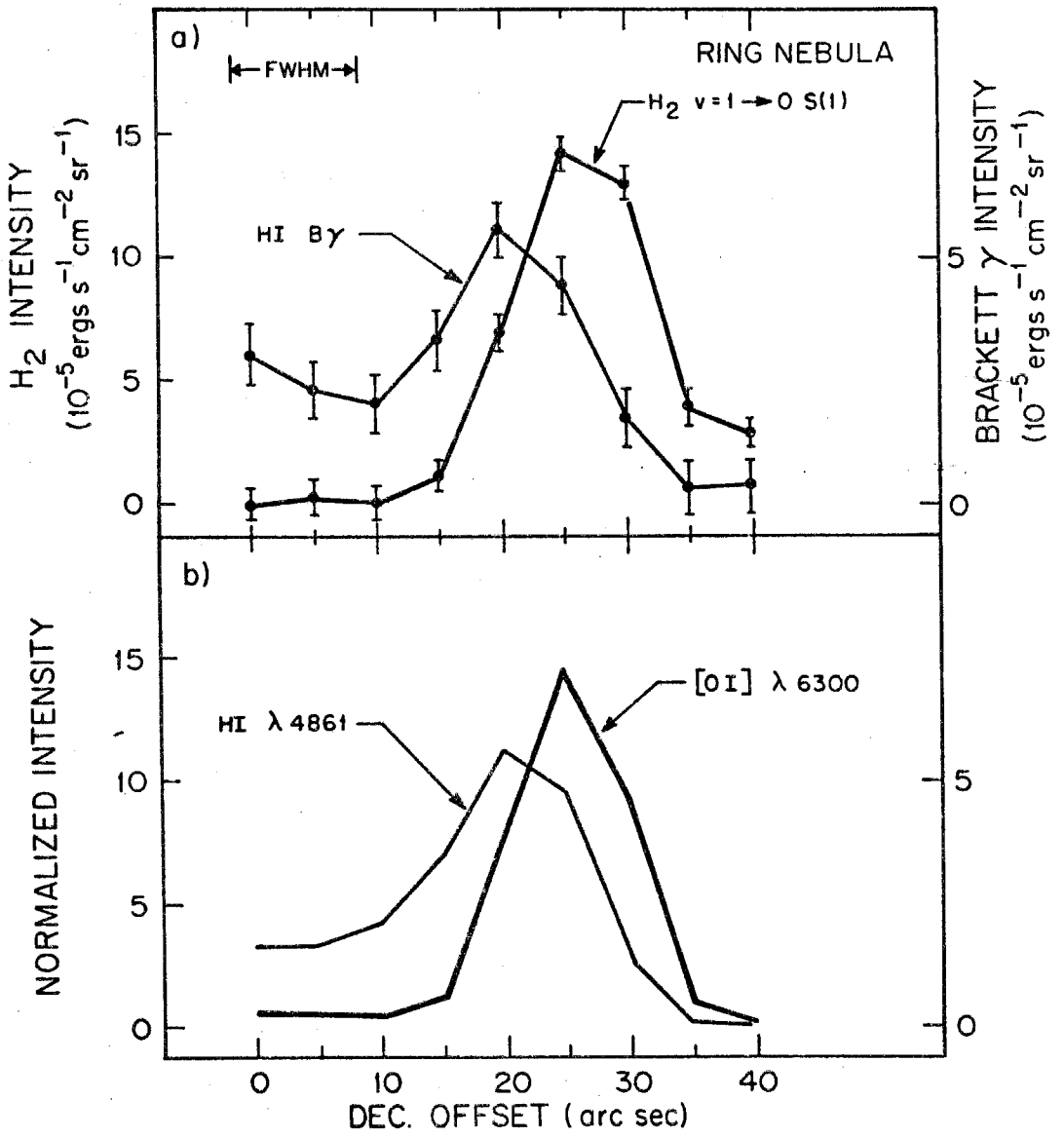
a)
RING NEBULA
←FWHM→
H2 v=1→0 S(1)
HI Bγ
H2 INTENSITY
(10^-5 ergs s^-1 cm^-2 sr^-1)
BRACKETT γ INTENSITY
(10^-5 ergs s^-1 cm^-2 sr^-1)
15
10
5
0
b)
HI λ4861
[OI] λ6300
NORMALIZED INTENSITY
0
10
20
30
40
DEC. OFFSET (arc sec)

Fig. 2

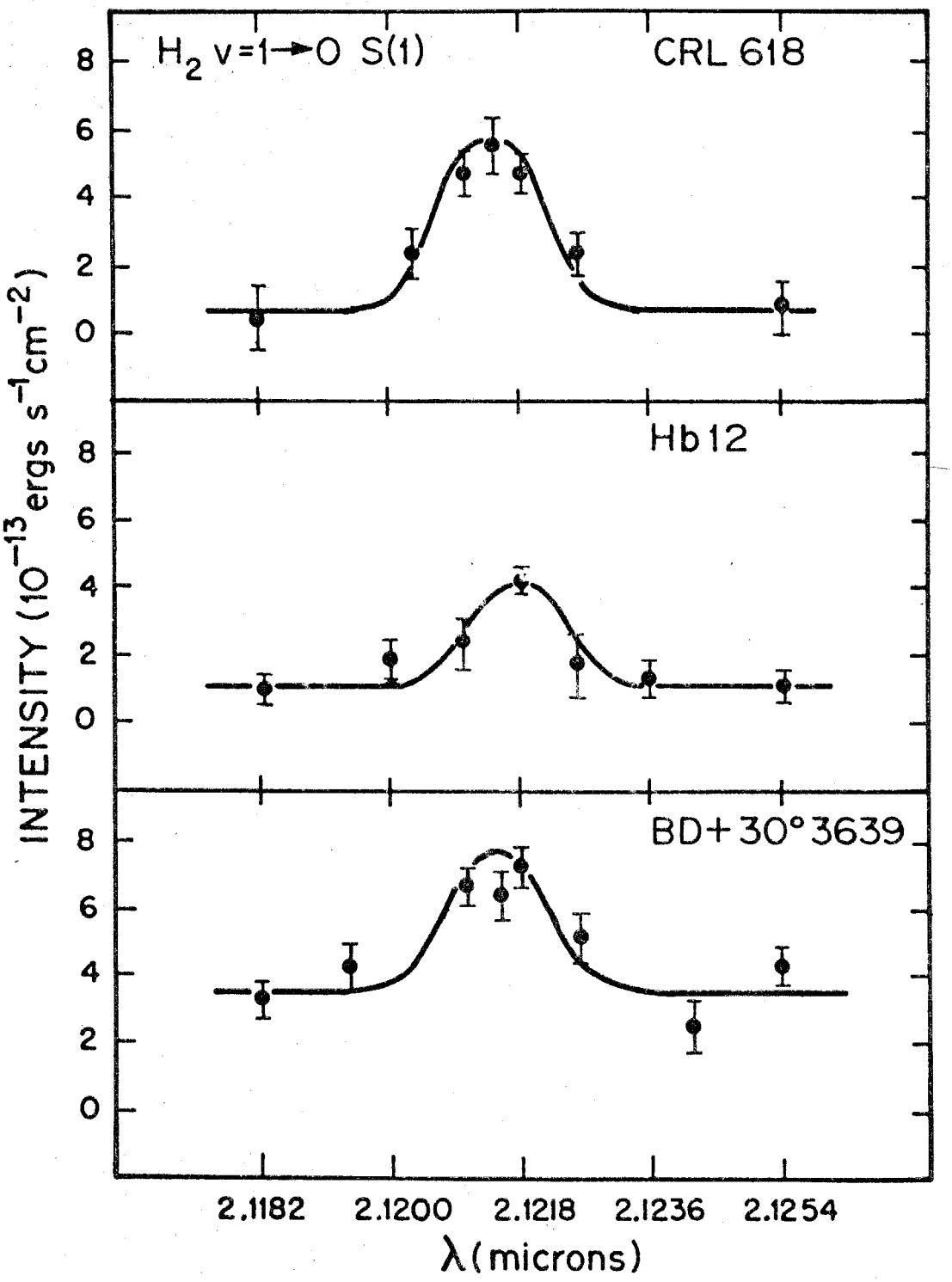
H2 v=1→0 S(1)
CRL 618
Hb 12
BD+30°3639
INTENSITY (10^-13 ergs s^-1 cm^-2)
0
2
4
6
8
2.1182
2.1200
2.1218
2.1236
2.1254
λ (microns)

Fig. 3

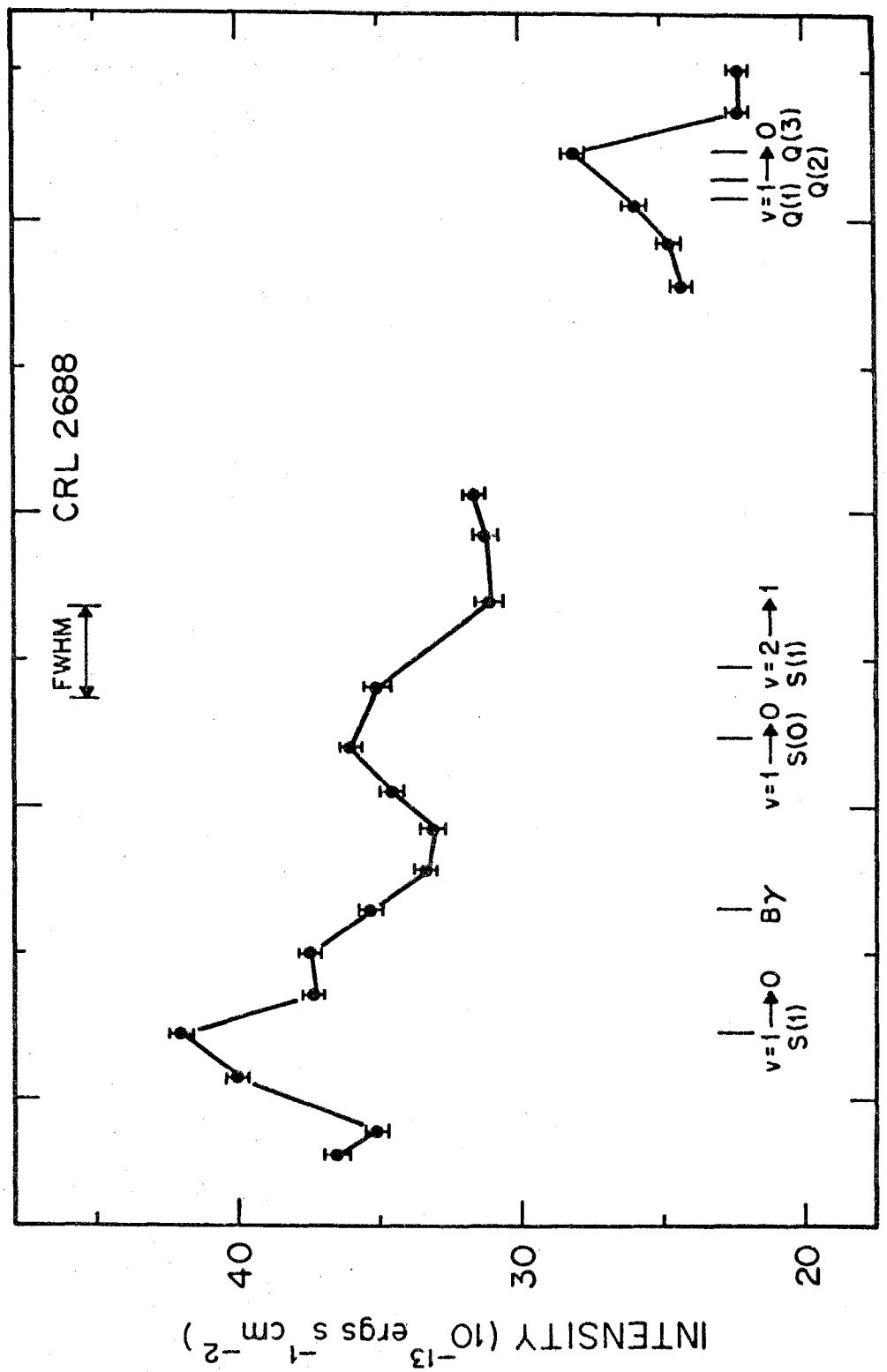
CRL 2688
FWHM
v=1→0 S(1)
Bγ
v=1→0 S(0)
v=2→1 S(1)
v=1→0 Q(1) Q(3) Q(2)
INTENSITY (10⁻¹³ ergs s⁻¹ cm⁻²)
λ (microns)
20
30
40
2.10
2.20
2.30
2.40

Fig. 4

PAPER 2:

MOLECULAR HYDROGEN EMISSION FROM T TAURI STARS

Submitted for publication to

the Astrophysical Journal

in collaboration with

I. Gatley, K. Matthews, and G. Neugebauer

I. INTRODUCTION

Molecular hydrogen emission has recently been detected from the Orion Nebula (Gautier et al. 1976), from planetary nebulae (Treffers et al. 1976; Beckwith, Persson, and Gatley 1978), and from the galaxy NGC 1068 (Thompson, Lebofsky, and Rieke 1978). Because this emission is not understood it may be useful to extend the range of observations to classes of objects other than those listed above. In this regard T Tauri stars are good candidates; they are often found in the vicinity of molecular clouds, and are emission line objects (see, e.g., Strom, Strom, and Grasdalen 1975).

We have searched for molecular hydrogen emission in the $v = 1 \rightarrow 0$ S(1) line at 2.12 μm in five T Tauri stars. In this Letter the observational results of this limited search are presented. The detection of H_2 emission in one of these objects satisfies our aim to find a new class of molecular hydrogen sources; however, the present observations do not bear directly on the problem of the excitation mechanism.

II. OBSERVATIONS

The observations were made using the 2.5 m Hooker telescope at Mount Wilson and the 5 m Hale telescope at Palomar Mountain during 1977 October and November. An Ebert-Fastie grating spectrometer with 17 Å

resolution was used throughout; the instrument and procedures for its use are described by Beckwith et al. (1978). For the present observations the focal plane diaphragm was generally 5" in diameter and the beam spacing was 30"; in the case of T Tau, measurements were also made with a 10" diaphragm and a 60" beam spacing for sky subtraction. No airmass corrections have been applied to the data.

Flux calibration was achieved by observations of β Per. The 2.1 μm flux density of this star is assumed to be 83 Jy, while the continuum is assumed to follow the Rayleigh-Jeans law in the 2 μm atmospheric window.

For each line seven wavelengths were observed; the wavelength of the $v = 1 \rightarrow 0$ S(1) line of H_2 measured in air (2.1213 μm), and wavelengths on each side of the line displaced 0.5, 1, and 2 times the spectrometer resolution element of 17 Å. In the case of T Tau positions centered 5" north, south, east and west were also measured with a 5" focal plane diaphragm; at these positions only the wavelength of the $v = 1 \rightarrow 0$ S(1) line and a representative continuum wavelength of 2.1255 μm were measured. For T Tau the $v = 2 \rightarrow$ S(1) line of H_2 and the Brγ line of atomic hydrogen were also measured; as for the H_2 line, seven wavelengths on and adjoining each line were observed.

III. RESULTS

Figure 1 shows the measured spectra in the vicinity of the $v = 1 \rightarrow 0$ S(1) line of H_2 for five T Tauri stars. Figure 1 also shows

measurements of T Tau made with both a 5" and a 10" focal plane diaphragm. The line strength in the former is $(3.1 \pm 0.4) \times 10^{-13}$ ergs s^{-2} cm^{-2} while that in the latter is $(5.7 \pm 1.0) \times 10^{-13}$ ergs s^{-1} cm^{-2}. The increase in line strength with increasing diaphragm size indicates that the emitting region is probably larger than 5"; this result is only marginally significant (2.5σ). Table 1 lists the measured line strengths at positions 5" north, south, east and west of T Tau; although the H_2 line was not positively detected at any of these positions, the upper limits on the line strengths are consistent with the increase seen between the 5" and 10" diaphragms. The emission is therefore probably centered on the star. No emission was detected in the other four stars shown; the line strengths are $< 1.3 \times 10^{-13}$ ergs s^{-1} cm^{-2} (3σ).

The $v = 2 \rightarrow 1$ S(1) line of H_2 was also searched for at wavelengths around 2.25 μm. No identifiable feature was observed in a 5" diaphragm; the 3σ upper limit on the line strength is 3×10^{-13} ergs s^{-1} cm^{-2}.

Figure 2 shows the spectrum of T Tau in the vicinity of the Bγ line of atomic hydrogen. The line is seen with a strength of 8×10^{-13} ergs s^{-1} cm^{-2}.

IV. DISCUSSION

The major results of this Letter are that molecular hydrogen emission is seen from T Tauri and that the region of emission is probably extended (> 5"). The strength of molecular hydrogen emission in T Tauri is at least three times greater than the strength of this emission

in any of the other T Tauri stars in the sample.

The excitation mechanism for the H_2 in T Tau cannot be determined from the present data. As in previously known cases of H_2 emission, we are confronted with a physical system in which several plausible alternatives for the excitation mechanism exist. From observations of atomic hydrogen lines, such as the present Bγ line measurement, it is known that some mechanism in the outer envelope of the T Tauri stars is capable of ionizing hydrogen. Therefore the H_2 molecules could possibly be excited by ultraviolet radiation or by electron collision in the interface between the ionized and neutral material. On the other hand, a high mass loss rate from T Tau may cause supersonic shocks in the surrounding neutral material (Schwartz 1975). It is possible that these shocks excite the H_2 in the manner proposed to explain the molecular hydrogen emission from the Orion nebula (Hollenbach and Shull 1977, Kwan 1977).

For the case of shock excitation it is possible to estimate from the observations the mass loss rate and neutral particle density in the shocked region. If the H_2 emission is assumed to come from an optically thin, uniform spherical surface 5" in diameter, then the surface brightness of the $v = 1 \rightarrow 0$ S(1) line is $\sim 3 \times 10^{-4}$ ergs s^{-1} cm^{-2} sr^{-1}. If we assume a 15 km s^{-1} shock velocity, Kwan's model for shock excitation, and this value for the surface brightness of the $v = 1 \rightarrow 0$ S(1) line,

then we find the density of molecular hydrogen in the preshocked region to be $\sim 2 \times 10^4$ cm^{-3}. With this density and shock velocity, the pressure necessary to push the shock continuously can be derived; the result is $\sim 10^{-7}$ dynes cm^{-2}. If this pressure is equated to the momentum per second associated with mass loss from the star and the velocity of the material is 200 km s^{-1}, then a mass loss rate of 5×10^{-8} $M_\odot$ yr^{-1} is required to sustain the shock. This result is of the same order of magnitude as mass loss rates derived by other means (Kuhi 1964, Schwartz 1975).

Differences between T Tau and the other stars in this sample may include the density of the neutral material surrounding the stars, the mass loss rate, or the ultraviolet luminosity of the emission line regions. Inasmuch as the mass loss rates for the two brightest stars in the sample, T Tau and RY Tau, are about the same (Kuhi 1964) and the Balmer lines are actually the strongest in HL Tau (Rydgren, Strom, and Strom 1976), we suggest that the density of surrounding material is the most critical factor for molecular hydrogen emission. In support of this suggestion are the observations of CO emission, which is relatively bright in the case of T Tau (Knapp et al. 1977), the presence of emission nebulosity associated with T Tau (Burnham 1890, 1894; Schwartz 1974), and the relative brightness of T Tau at far infrared wavelengths (Harvey, Thronson, and Gatley 1979).

Unfortunately, cloud densities, mass loss rates, and ultraviolet luminosities are not well known for the stars in our sample. It is therefore not possible to come to any definite conclusions about the

brightness of H_2 emission in T Tau relative to other T Tauri stars. Despite the difficulties in interpreting the data we have presented, it is likely that further spectroscopic studies of T Tauri stars will be a fruitful source of information about molecular hydrogen emission and the star formation process.

TABLE 1

FLUX MEASUREMENTS OF THE $v = 1 \rightarrow 0$ S(1) LINE NEAR T TAU

	5" North	5" East	5" South	5" West
Line Flux (10^{-13} ergs s^{-1} cm^{-2})	0.6 ± 0.6	0.4 ± 0.4	-0.1 ± 0.6	0.6 ± 0.6

REFERENCES

Beckwith, S., Persson, S. E., and Gatley, I. 1978, Ap. J. (Letters) 219, L33.

Beckwith, S., Persson, S. E., Neugebauer, G., and Becklin, E. E. 1978, Ap. J., in press.

Burnham, S. W. 1890, M.N.R.A.S., 51, 94.

_____. 1894, Pub. Lick. Obs., 2, 175.

Gautier, T. N. III, Fink, U., Treffers, R. P., and Larson, H. P. 1976, Ap. J. (Letters), 207, L129.

Harvey, P. M., Thronson, H. A., and Gatley, I. 1979, in preparation.

Hollenbach, D. J., and Shull, J. M. 1977, Ap. J., 216, 419.

Knapp, G. R., Kuiper, T.B.H., Knapp, S. L., and Brown, R. L. 1977, Ap. J., 214, 78.

Kuhi, L. V. 1964, Ap. J., 140, 1409.

Kwan, J. 1977, Ap. J., 216, 713.

Rydgren, A. E., Strom, S. E., and Strom, K. M. 1976, Ap. J. Suppl., 30, 307.

Schwartz, R. D. 1974, Ap. J., 191, 419.

_____. 1975, Ap. J., 195, 631.

Strom, S. E., Strom, K. M., and Grasdalen, G. 1975, Ann. Rev. Astron. and Astrophys., 13, 187.

Thompson, R. I., Lebofsky, M. J., and Rieke, G. H. 1978, preprint.

Treffers, R. R., Fink, U. Larson, H. P., and Gautier, T. N. III 1976, Ap. J., 209, 793.

FIGURE CAPTIONS

Figure 1. The spectra of five T Tauri stars at the position of the $v = 1 \rightarrow 0$ S(1) line of molecular hydrogen. In each case the two longest and two shortest wavelengths are used to define the continuum level indicated. For the spectrum of T Tau the measured instrumental profile, arbitrarily normalized, has been roughly fit to the data. Except for the "T Tau 10" spectrum" the observations were made with a 5" focal plane diaphragm.

Figure 2 The spectrum of T Tau at the position of the Bγ line of atomic hydrogen as measured with a 5" focal plane diaphragm. The continuum level indicated was defined by the two longest and two shortest wavelengths measured. The measured instrumental profile, arbitrarily normalized, has been roughly fit to the data.

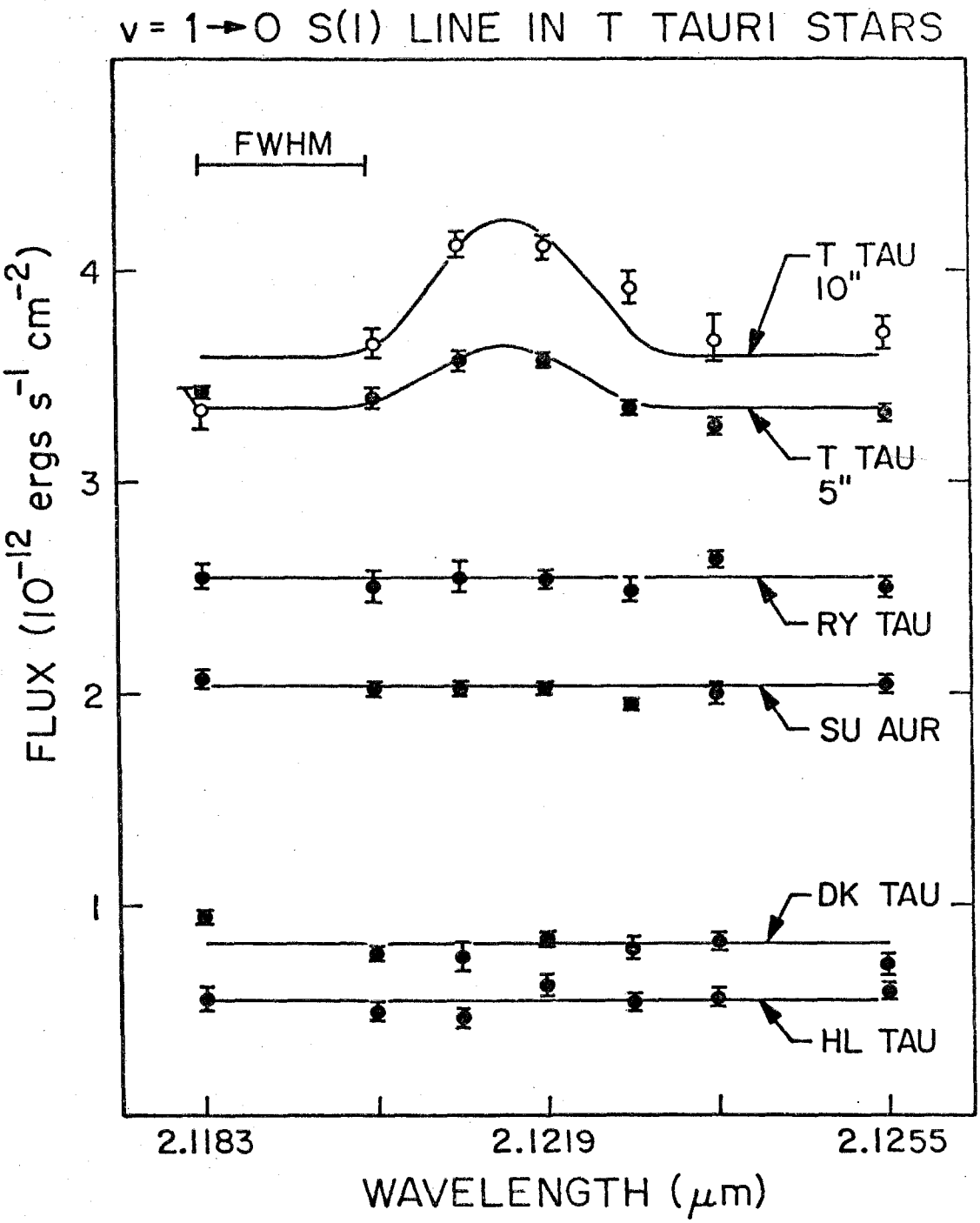
v = 1→0 S(1) LINE IN T TAURI STARS
FWHM
T TAU 10"
T TAU 5"
RY TAU
SU AUR
DK TAU
HL TAU
FLUX (10^{-12} ergs s^{-1} cm^{-2})
4
3
2
1
2.1183
2.1219
2.1255
WAVELENGTH (μm)

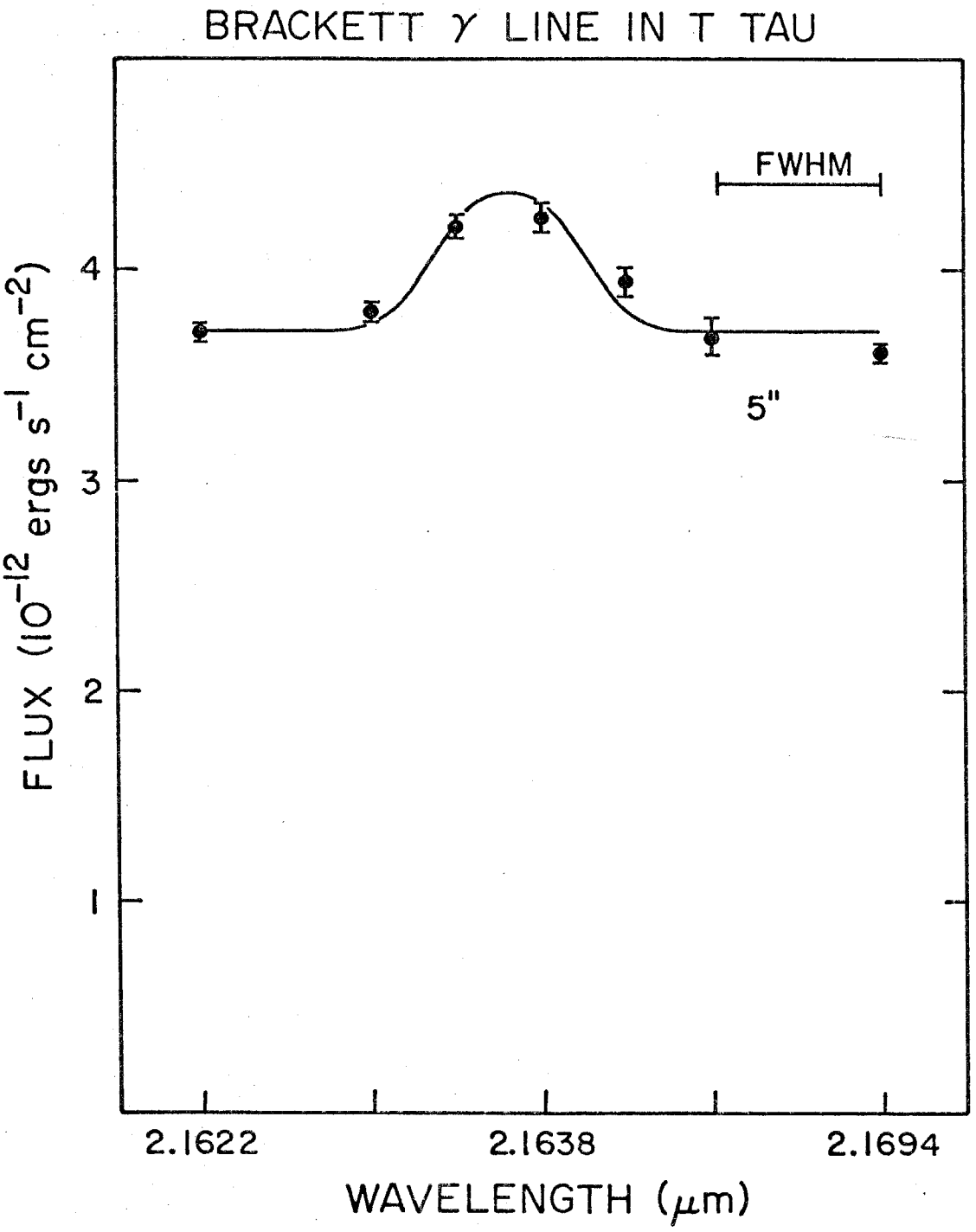
BRACKETT γ LINE IN T TAU
FWHM
5"
FLUX (10^{-12} ergs s^{-1} cm^{-2})
4
3
2
1
2.1622
2.1638
2.1694
WAVELENGTH (μm)

PAPER 3:

OBSERVATIONS OF THE MOLECULAR HYDROGEN EMISSION FROM THE ORION NEBULA

Submitted for publication to

the Astrophysical Journal

in collaboration with

S. E. Persson, G. Neugebauer, and E. E. Becklin

I. INTRODUCTION

Near infrared emission from molecular hydrogen has been detected in the direction of the infrared cluster in Orion by Gautier et al. (1976) and studied by Grasdalen and Joyce (1976). Molecular hydrogen emission has also been detected from NGC 7027 by Treffers et al. (1976) and from five planetary nebulae by Beckwith, Persson and Gatley (1978).

In this paper new observations of the emission from molecular hydrogen in the Orion nebula are presented. Maps at 13" and 5" resolution have been made which clarify the extent and structure of the emission. Accurate line ratio measurements have also been obtained, and from these temperatures and column densities are derived. The new data are used to discuss possible excitation mechanisms for the H_2 emission.

II. OBSERVATIONS

All the observations presented in this paper were made at the Cassegrain foci of the 2.5 meter reflector at Mt. Wilson and the 5 meter Hale reflector at Palomar Mountain. A 0.5 m focal length Ebert-Fastie grating spectrometer was used for all the observations. The instrumentation, wavelength calibration, and standards to which the measurements are referred are described in Appendix A.

a) Mapping in the $v = 1 \rightarrow 0$ S(1) Line

A map with 13" resolution of the emission from the $v = 1 \rightarrow 0$ S(1) transition of H_2 (2.1218 μm) was made in 1976 October using the

2.5 meter reflector with the single detector system (see Appendix A). The result is shown in Figure 1. The entrance aperture was circular, the spectral resolution was 20 Å (4.4 cm^{-1}), and the incoming signal was chopped against an ambient temperature blackbody. The measurements were made by changing the grating angle every 40 seconds so the detector saw first the wavelength of the line and then alternately wavelengths offset 36 Å (8 cm^{-1}) to each side of the line wavelength. The total integration time at each point on the sky was 160 seconds -- 80 seconds at the line wavelength and 40 seconds at each of the two continuum wavelengths.

The line strengths were measured on a grid of points spaced 10" apart on the sky. The positions of the points were measured relative to that of the Becklin-Neugebauer (BN) source (see Wynn-Williams and Becklin 1974); the uncertainty in the absolute position of the map is ± 3" (1σ). On the basis of the known transmission of the earth's atmosphere (Hall 1974) the air mass correction at 2.12 μm was assumed to be negligible; no observations were made at an air mass greater than 2.

A map of the H_2 emission with 5" resolution was made in the $v = 1 \rightarrow 0$ S(1) transition in 1976 November, 1976 December, and 1977 February on the 5 meter Hale reflector; it is shown in Figure 2. For all the mapping a circular aperture was used and the signal was chopped against an ambient temperature blackbody. Most of the mapping was done with the single detector system operated at a wavelength resolution of 17 Å (3.8 cm^{-1}). Approximately one third of the map in Figure 2 was made

with the double detector system described in Appendix A. One fourth of this mapping overlapped that done with the single detector system; the results are in good agreement.

The map was made by measuring a grid of points spaced 2.5" apart on the sky within the limits given by the boundary drawn in Figure 2. The telescope was pointed by offsetting from the position of the BN source; the resulting positional accuracy is probably better than ± 2". The total integration time per point varied somewhat in different portions of the map, but was typically 160 seconds.

b) Measurements of Line Ratios

Table 1 gives the intensity measurements of molecular hydrogen lines measured in the Orion nebula; Figure 3 shows four of the lines measured on Pk 1. The $v = 1 \rightarrow 0$ S(0), S(1), S(2) and Q(3), and the $v = 2 \rightarrow 1$ S(1) transitions of H_2 were measured on Pk 1 and Pk 2 in 1976 December using the 2.5 meter reflector. For all the line intensity measurements a 10" aperture was used; for those measured on Pk 1 and Pk 2 sky subtraction was accomplished with a 1' beam spacing. In the case of Pk 1, measurements of the $v = 1 \rightarrow 0$ S(0), S(1), and $v = 2 \rightarrow 1$ S(1) transitions were also made by chopping against an ambient temperature blackbody. From these measurements it was determined that no significant error resulted from sky subtraction.

The observations of line intensities were made using the single detector system at seven wavelengths, four off the line wavelength to establish a continuum baseline, two at the half power wavelengths

of the instrumental profile to check centering, and one midway between the half power wavelengths to measure the line strength. As this was done for each line no significant error can accrue from velocity gradients in the source or wavelength calibration shifts from point to point on the sky.

Air mass corrections were taken to be zero for all the line transitions. For the $v = 1 \rightarrow 0$ Q(3) line the extinction depends strongly on the water vapor content of the atmosphere at the time of the measurements as well as the relative velocity between the earth and the source. Since neither of these quantities was well determined, the data on the Q(3) line have been assigned a 30% uncertainty.

III. RESULTS

a) Mapping

Figure 1 shows the map of the $v = 1 \rightarrow 0$ S(1) emission close to the near infrared cluster in Orion. The peak surface brightness agrees well with that of Grasdalen and Joyce (1976), but the detailed shape and location of emission on the present map differs from theirs. In particular, the emission peak southeast of the BN source does not appear on their map. Since the boundary of the mapped area is given by the outermost contour where the surface brightness is about one tenth that of Pk 2, the emission region is larger than that shown

in Figure 1. In addition, the v = 1 → 0 S(1) line was detected with a line strength of (1.2 ± 0.3) x 10^{-4} ergs s^{-1} cm^{-2} sr^{-1} in a 13" aperture at a point 20" west of θ^2 Ori A; this point lies on the ridge of near infrared emission reported by Becklin et al. (1976).

The luminosity in the v = 1 → 0 S(1) line of the region mapped in Figure 1 is 2.5 $L_\odot$ if no correction is made for interstellar extinction. If all the molecules are assumed to be at a temperature of 2000 K (see below) the contribution of other lines to the total molecular hydrogen luminosity can be calculated to be ~ 50 $L_\odot$ if extinction is neglected.

Both regions of line emission maxima, as determined from Figure 1, are close to infrared continuum sources. The southernmost region coincides with the continuum source found at 10 μm by Gehrz, Hackwell and Smith (1975) and the northern region is near the unresolved near infrared source IRS 2 found by Hilgeman (1970) at 2.2 μm and shown on the map of Wynn-Williams and Becklin (1974). There is no enhancement of molecular hydrogen emission in the immediate vicinity of the BN and Kleinmann-Low (KL) sources. The centroid of the H_2 emission lies within ~ 10" of the centroid of the high velocity J = 3 → 2 CO emission found by Phillips et al. (1977) but the distribution of H_2 emission as given in Figure 1 is not reproduced by their data. The general shape and extent of the emission are not correlated with those in the high spatial resolution radio continuum map at 5 GHz of Gull and Martin (1975).

With the higher resolution data of Figure 2 it can be seen that there is substantial structure in the line emission as evidenced by

five emission peaks identified on the map. The positions of these peaks and the measured surface brightnesses are given in Table 1. It is seen that the ratios of the various H_2 line intensities are the same on Pk 1 and Pk 2 within the uncertainties and furthermore, where measured, are independent of position on the map. This is one of the basic observational results of this work.

It is of interest that the northernmost source seen in Figure 1 splits up into two components, neither of which is coincident with the continuum source IRS 2. Comparison of the 5" resolution map with data on various compact radio, infrared, and optical sources shows that no detailed spatial correlation exists between the H_2 surface brightness and the various sources. In particular, the H_2O maser positions of Genzel and Downes (1977), the infrared source positions given by Wynn-Williams and Becklin (1974) and Gehrz, Hackwell and Smith (1975), and the photograph in the [OI] λ6300 line of Münch and Taylor (1974) do not show overall detailed correlations with the surface brightness of H_2 emission. A 1 μm photograph of the region shows no features coincident with any of the peaks of H_2 emission. Maps of other molecular lines have too low a spatial resolution to be compared with the data presented here.

IV. DISCUSSION

In this section the new data are used to make simple estimates of the temperatures of the emission region and the power requirements for the source or sources of energy that excite H_2 molecules.

a) Physical Parameters

The column densities N(v,J) of the molecules in the level (v,J) can be derived for the upper levels of the observed transitions independently of the excitation mechanism. For optically thin emission the intensity of a particular transition is given by

$$I = Ah\nu N(v,J)/4\pi$$

where A is the Einstein A value of the transition and $h\nu$ is the photon energy. Table 2 lists the derived column densities for Pk 1 and Pk 2 using the values of A and $h\nu$ given by Gautier et al. (1976) for the $v = 1 \rightarrow 0$ transitions. The assumed A value for the $v = 2 \rightarrow 1$ S(1) transition is 5.0×10^{-7} sec^{-1} (Turner, Kirby-Docken, and Dalgarno 1977) and the corresponding frequency is computed using the spectroscopic constants given by Fink, Wiggins, and Rank (1965). For an optical depth of unity in these transitions, column densities of $\sim 10^{26}$ cm^{-2} are required. The derived column densities are $\sim 10^{8}$ times smaller and therefore the emission is optically thin.

If the level populations are in a Boltzmann distribution and the molecules are excited by collisions,

$$\ln[N(v,J)/g_J] = -E/kT + \text{const.}$$

where g_J is the statistical weight for the (v,J) level and E is the energy of the level above the ground state. The additive constant is independent of E. Figure 4 shows a plot of $\log [N(v,J)/g_J]$ vs E for the $v = 1 \rightarrow 0$ S(0), S(1) and S(2), and $v = 2 \rightarrow 1$ S(1) transitions on Pk 1 and Pk 2. The data from the $v = 1 \rightarrow 0$ Q(3) transition have not been incorporated in the plot because of the large measurement uncertainty.

Both vibrational and rotational temperatures can be derived from the data; Gautier et al. (1977) derived a rotational temperature of 2500 K (+1500 K, -700 K) in the direction of the BN source. The slopes of the lines drawn in Figure 4 yield a vibrational temperature of $\sim$ 2200 $\pm$ 220 K. A rotational temperature of 1100 $\pm$ 150 K is derived from the v = 1 levels alone. The data plotted in Figure 4 display only the calibration and statistical uncertainties; if uncertainties in the A values are taken into account, the uncertainty in the vibrational temperature becomes $\pm$ 300 K.

Only the J = 3 level for the two different vibrational levels has been used to derive the vibrational temperature. This temperature must be corrected for reddening as discussed below since the $v = 2 \rightarrow 1$ S(1) and $v = 1 \rightarrow 0$ S(1) lines are at different wavelengths and differential extinction will change the observed line ratio. If, instead, the $v = 1 \rightarrow 0$ S(0) line is used with the $v = 2 \rightarrow 1$ S(1) line the effects of reddening are negligible since these two lines occur at almost the same wavelength. The derived vibrational temperature is then 2000 K. This method assumes that the rotational and vibrational temperatures are equal and the ortho to para hydrogen ratio is 3 to 1.

The largest uncertainty in determining the temperature arises from the lack of knowledge of the extinction to the H_2 emission. If the extinction at 2 μm is as large as 3 mag the corrected rotational temperature is 2000 K at Pk 1. The corrected vibrational temperature for this amount of extinction at Pk 1 is 1960 K. This amount of extinction is reasonable for sources in the Orion Molecular Cloud as

given by Thaddeus et al. (1971); Becklin, Neugebauer, and Wynn-Williams (1973); and Grasdalen and Joyce (1976). Because uncertainties in the extinction to the H_2 create substantially larger uncertainties in the rotational temperature than in the vibrational temperature, we will take the vibrational temperature to be representative of the actual temperature of the H_2.

Column densities of all the H_2 molecules can be derived from the line intensity measurements and the calculated temperature. In a Boltzmann distribution, the level populations are given by

$$N(v,J) = N_{H_2} g_j e^{-E/kT}/Q(T)$$

where $Q(T)$ is the partition function and N_{H_2} is the total H_2 column density. This formula has been used to compute the values of N_{H_2} listed in Table 1 by assuming the temperature at all the peaks to be 2000 K. The column densities at the peaks are all of order 10^{19} cm^2.

It is of interest to see if the conditions necessary for the molecules to be in a Boltzmann distribution obtain for the region under consideration. A necessary condition is that the time between collisions be shorter than the radiative lifetime of any level. The collision rate per molecule is given by

$$R_c \simeq n_{H_2} \sigma_c v_{th} \sim 5 \times 10^{-14} n_{H_2} \sqrt{T} \ s^{-1}$$

where n_{H_2} is the volume density of H_2 molecules (cm^{-3}), σ_c is the H_2-H_2 collision cross section, v_{th} is the molecular thermal velocity, and the temperature T is measured in degrees Kelvin. The radiative rates for the relevant levels are $\sim 10^{-6}$ s^{-1} and σ_c is on the order of 10^{-18} cm^2 for collisions which change the vibrational quantum

number. If T is taken to be 2000 K, the relation above indicates that collisions are dominant for $n_{H_2} \gtrsim 10^6$ cm^{-3}. This is consistent with lower limits to the volume density of $\sim 10^5$ cm^{-3} derived from measurements of other molecules in the same direction (Kutner et al. 1971, Liszt et al. 1974), and thus conditions for the molecules to exist in a Boltzmann distribution can be satisfied. Note that the cross sections for collisions which change the rotational quantum number of the molecules will in general be larger than those which change the vibrational quantum number, and thus a Boltzmann distribution should be established among levels with the same vibrational quantum number at lower densities and temperatures than are necessary to establish this distribution among all the levels. We have used the cross sections necessary for thermalization of the observed vibrational levels.

If the surface brightness of the H_2 is roughly uniform over the resolution element of the observations, then the thickness of the emitting region is $\lesssim 10^{14}$ cm (3×10^{-5} pc) for a column density of $\sim 10^{19}$ cm^{-2} and volume density $\gtrsim 10^5$ cm^{-3}. This is 10^{-4} times the projected size of the emission on the sky of ~ 0.3 pc. Even if the volume density is only $\sim 10^3$ cm^{-3} the thickness of the emitting region is very small in comparison with the size of the region. We conclude that the H_2 exists in a thin, hot sheet. This conclusion was also reached by Grasdalen (1976).

b) Energy Sources

Shock excitation of the H_2 has been suggested by Gautier et al. (1976) and Kwan and Scoville (1976) to explain the H_2 emission. Since

then, several detailed calculations have been made which support this possibility (Hollenbach and Shull 1977; London, McCray, and Chu 1977; Kwan 1977). The model calculations give limits to the shock velocity and volume densities of molecular hydrogen in the preshocked material required to produce the observed line intensities. Kwan (1977) derives a lower limit of $\sim$ 10 km s^{-1} for the shock velocity required to produce the observed temperature of 2000 K. From the observed intensity of the $v = 1 \rightarrow 0$ S(1) line the minimum average H_2 volume density n_{H_2} is $\sim 10^5$ cm^{-3} if shock excitation obtains (see e.g., Kwan 1977). Any correction to the $v = 1 \rightarrow 0$ S(1) line intensity to account for extinction at 2.1 μm will raise n_{H_2} proportionally.

From the values of density and velocity, the minimum pressure necessary to sustain the shock is $\sim 3 \times 10^{-7}$ dynes cm^{-2}. There is no observed source in the region that can drive such a shock continuously by exerting pressure on the molecular cloud (see e.g., Kwan 1977 or Hollenbach and Shull 1977). In particular, the H II region cannot provide enough pressure nor can any luminosity source or combination of luminosity sources in the Orion Molecular Cloud. If the H_2 is shock excited the shock must have been the result of an energetic explosion such as that from a supernova as suggested by Kwan and Scoville (1976).

An immediate conclusion that can be drawn from the data presented above is that the level populations are not determined by pure

radiative excitation and cascades as calculated by Black and Dalgarno (1976). In particular, Black and Dalgarno predict a ratio of $(v = 1 \rightarrow 0\ S(1))(v = 2 \rightarrow 1\ S(1)) = 1.8$ whereas the measured value is 10. Gautier et al. (1976) have reached a similar conclusion based on their upper limit for the $v = 2 \rightarrow 1\ S(1)$ line. It may be possible for radiative excitation to provide the energy input to the molecules, but in this case collisions or some other process must redistribute the level populations so as to give the observed line ratios. No detailed mechanism has been proposed which can easily redistribute the level populations except for that of resonant H_2-H_2 collisions as discussed by Shull (1978). The effectiveness of this mechanism is not known. The most likely candidate to provide the radiation energy would be θ^1 Ori (C). This star has just enough luminosity to provide the necessary energy input only if all of the energy can be put into the $v = 1$ level with close to unit efficiency. If the visual extinction is as high as 3 mag, then θ^1 Ori (C) could not provide the necessary energy and radiative excitation would be extremely unlikely.

We have not considered the possibility that the H_2 is powered by the release of energy during gravitational collapse of the cloud material. It is very unlikely that a temperature of 2000 K could be generated in a sheet during a collapse of the entire cloud. If, instead, the emission arises from the collapse of many small regions

we might expect each peak in the H_2 emission to be associated with an infrared continuum source or protostar. Our data do not show a detailed correlation to exist between H_2 emission and infrared continuum emission at 2 μm although the continuum data are not particularly sensitive and sources may be masked by extinction.

V. SUMMARY AND CONCLUSIONS

From the observations presented in this paper the basic properties of the molecular hydrogen emission in the Orion nebula are the following:

1) As shown in Figures 1 and 2, the spatial extent of the emission is on the order of 2' x 2' with several localized emission peaks. The highest surface brightness of emission in the $v = 1 \rightarrow 0$ S(1) transition is 8.5×10^{-3} ergs s^{-1} cm^{-2} sr^{-1}. The total luminosity of the Orion source is 2.5 $L_\odot$ in this transition alone. The centroid of the emission corresponds approximately with the positions of the BN/KL infrared cluster. The detailed structure of the H_2 emission does not correlate with the position of other types of emission from this region.

2) The excitation temperature, as determined from the ratio of the intensities of the $v = 2 \rightarrow 1$ S(1) and $v = 1 \rightarrow 0$ S(1) transitions, is 2000 ± 300 K. The same temperature is observed on the two brightest emission peaks shown in Figure 1. None of the line ratios measured at any place in the emission region show evidence for deviations from this temperature.

3) If the H_2 level populations are in a Boltzmann distribution the average H_2 column density is $\sim 10^{19}$ cm^{-2}.

Based on these results, several conclusions regarding the molecular hydrogen emission can be drawn.

1) The hydrogen probably exists in a sheet $\leq 10^{14}$ cm thick.

2) Pure radiative excitation and subsequent fluorescence as discussed by Black and Dalgarno (1976) is not responsible for the emission since the observed line ratios are substantially different from those predicted by this mechanism.

3) There is not enough energy density either in the H II region or in the observed luminosity sources in the region to provide for shock excitation of the H_2. Thus, if the H_2 is shock heated, the shock must have resulted from a cataclysmic event such as a supernova explosion.

APPENDIX A

a) Instrumentation

All measurements presented in this paper were made with the Ebert-Fastie spectrometer of 0.5 m focal length described by McCammon, Münch, and Neugebauer (1967). A 600 groove mm^{-1} grating is used at ambient temperature and gives a dispersion of 33 Å mm^{-1} in first order at 2.1 μm. An important modification to the system beyond that described by McCammon et al. (1967) is that a barium fluoride lens is used to convert the incoming f/16 beam from the telescope to f/5 for the spectrometer. This allows for entrance apertures less than 0.5 mm in diameter to be used in the spectrometer without requiring extremely high spatial resolution on the sky. Thus spectral resolution is preserved and a large gain in signal for extended sources is

achieved. The f/5 beam out of the spectrometer is converted back to f/16 and enters an InSb detector system. Narrow band ($\Delta\lambda \sim 0.08$ μm) interference filters are used to reduce the background radiation from the spectrometer.

A focal plane chopper is used to chop the incoming beam between two different parts of the sky for sky subtraction or between the sky and a reference blackbody at the ambient temperature. The chopping mirror reflects light not entering the spectrometer during each half-cycle into a broadband (2.0-2.4 μm) detection system. This system is used for peaking up on 2 μm continuum sources which serve as positional reference points for the maps.

For the map with 5" resolution two separate detector systems were used for different parts of the map. One detector system uses a single detector which senses light from a single portion of the spectrum and whose wavelength resolution is determined by the entrance and exit apertures of the spectrometer. Subsequently, a two detector system was put into operation. One detector senses light from a single portion of the spectrum as in the initial system and the other senses light from portions of the spectrum directly adjacent to and at both longer and shorter wavelengths than that of the first detector. In a typical observation, the grating angle is set to center the line wavelength in the "line" channel of the two detector system, and the continuum on either side of the line in the continuum channel. The centers of the line and continuum channels are 17 Å apart. Wavelength resolution of the "signal" channel is 20 Å and resolution in the adjacent wavelengths is approximately

15 Å. The detector outputs are always adjusted so that the response to a strong continuum source is the same for each. The signals from the two detector channels are then subtracted to give a direct measure of the line strength. In this way mapping around a strong continuum source such as BN can be accomplished without incurring errors in the line strength due to fluctuations in seeing conditions and guiding error.

The flux was calibrated by observing α Leo and β Aur with 20 Å resolution at 2.1218 μm. The fluxes of these stars as determined from measurements relative to α Lyr were 150 and 120 Jy at 2.1218 μm; the flux of α Lyr at 2.2 μm is taken as 620 Jy and its spectrum is assumed to be Rayleigh-Jeans. The uncertainty in the overall flux calibration at each wavelength is estimated to be 10% for the $v = 1 \rightarrow 0$ S(0), S(1), S(2) and $v = 2 \rightarrow 1$ S(1) transitions and 30% for the $v = 1 \rightarrow 0$ Q(3) transition.

b) Wavelength Calibration

The spectrometer wavelength scale was calibrated at the telescope by observing the argon lines at 2.0616 μm, 2.0986 μm, 2.1534 μm, and 2.2077 μm from a laboratory argon lamp. Identifications of the H_2 lines were then made using the wavelengths given in Fink, Wiggins, and Rank (1965). For the $v = 2 \rightarrow 1$ S(1) transition the wavelength was calculated using the empirical constants of Fink, Wiggins, and Rank. The calculated wavelength for this transition is 2.2477 μm (4449.0 cm^{-1}).

The precise grating angle corresponding to the wavelength of the $v = 1 \rightarrow 0$ S(1) transition was determined relative to the four lines of argon by measuring the instrumental response versus grating angle on the

line at the position of greatest line brightness in Orion. The line wavelength could then be set by measuring the four argon lines and offsetting the grating angle relative to them. This was done before, during, and after mapping each night and the wavelength calibration was found to be constant to within 2 Å (0.4 cm^{-1}) or 30 km s^{-1} at the source. From the instrumental profile it is estimated that a wavelength shift of $\sim$ 2.5 Å or 38 km s^{-1} at the source is required to produce a 10% change in the measured line intensity.

For the measurements of the different H_2 lines the grating angles were calculated from the spectrometer wavelength calibration and the known grating angle for the $v = 1 \rightarrow 0$ S(1) transition.

TABLE 1

INTENSITIES OF H_2 LINES IN THE ORION NEBULA

Location	Right Ascension (1950)	Declination (1950)	Intensities (10^{-4} ergs s^{-1} cm^{-2} sr^{-1})*					Column† Density
			v = 1→0 S(0) 2.2233+	v = 1→0 S(1) 2.1218+	v = 1→0 S(2) 2.0338+	v =1→0 Q(3) 2.4237+	v = 2→1 S(1) 2.2477+	N_{H_2} (10^{18} cm^{-2})
Pk 1	$5^h32^m46^s.2$	-5°24'02"	20	75	25	90±30	7.2	22
Pk 2	$5^h32^m48^s.3$	-5°24'34"	13	50	16	50±20	5.2 ± 0.7	15
Pk 3	$5^h32^m47^s.3$	-5°24'26"	...	33	...	25± 8	...	9.7
Pk 4	$5^h32^m46^s.2$	-5°24'27"	9.4	32	...	...	...	9.4
Pk 5	$5^h32^m46^s.4$	-5°23'50"	...	...	...	...	...	...
BN	$5^h32^m46^s.7$	-5°24'17"	7 ± 1.5	30	...	...	...	8.8

*Uncertainties in all intensity measurements are ± 10% when not shown.

†Uncertainty in the column densities depends on the validity of the assumption that the populations are Boltzmann distributed. If this assumption is valid, the uncertainties are estimated to be ± 20%.

+Vacuum wavelength in μm.

TABLE 2

COLUMN DENSITIES N(v,J) OF
VIBRATIONALLY EXCITED UPPER LEVELS OF H_2

Upper Level	Transition Used	Pk 1 (cm^{-2})	Pk 2 (cm^{-2})
v = 1, J = 2	v = 1 → 0 S(0)	1.1×10^{17}	7.4×10^{16}
v = 1, J = 3	v = 1 → 0 S(1)	2.8×10^{17}	1.8×10^{17}
v = 1, J = 4	v = 1 → 0 S(2)	7.2×10^{16}	4.6×10^{16}
v = 2, J = 3	v = 2 → 1 S(1)	2.1×10^{16}	1.5×10^{16}

Note: Uncertainties in the column densities of the upper levels depend only on the measurement errors, and hence are all ± 10% except for v = 2, J = 3 on Pk2 (± 14%, see Table 1)

REFERENCES

Becklin, E. E., Beckwith, S., Gatley, I., Matthews, K., Neugebauer, G., Sarazin, C., and Werner, M. W. 1976, Ap. J., 207, 770.

Becklin, E. E., Neugebauer, G., and Wynn-Williams, C. G. 1973, Ap. J. (Letters), 182, L7.

Beckwith, S., Persson, S. E., and Gatley, I. 1978, Ap. J. (Letters), 219, L

Black, J. H. and Dalgarno, A. 1976, Ap. J., 203, 132.

Fink, U., Wiggins, T. A., and Rank, D. H. 1965, J. Mol. Spec., 18, 384.

Gautier, T. N. III, Fink, U., Treffers, R. P., and Larson, H. P. 1976, Ap. J. (Letters), 207, L129.

Gehrz, R. D., Hackwell, J. A., and Smith, J. R. 1975, Ap. J. (Letters), 202, L33.

Genzel, R. and Downes, D. 1977, Astr. Ap., 61, 117.

Grasdalen, G. L. 1976, private communication.

Grasdalen, G. L. and Joyce, R. R. 1976, B.A.A.S., 8, 349.

Gull, S. and Martin, A. 1975, Lecture Notes in Physics, Vol. 42, "H II Regions and Related Topics," ed. by T. L. Wilson and D. Downes, p. 369.

Hall, D. N. B. 1974, An Atlas of Infrared Spectra of the Solar Photosphere and of Sunspot Umbrae, (Tucson: Kitt Peak National Observatory).

Hilgeman, T. 1970, Ph.D. Thesis, California Institute of Technology.

Hollenbach, D. J. and Shull, J. M. 1977, Ap. J., 216, 419.

Kwan, J. 1977, Ap. J., 216, 713.

Kwan, J. and Scoville, N. 1976, Ap. J. (Letters), 210, L39.

Kutner, M., Thaddeus, P. Jefferts, K. B., Penzias, A. A., and Wilson, R. W. 1971, Ap. J. (Letters), 164, L49.

Liszt, H. S., Wilson, R. W., Penzias, A. A., Jefferts, K. B., Wannier, P. G., and Solomon, P. M. 1974, Ap. J., 190, 557.

London, R., McCray, R., and Chu, S. I. 1977, Ap. J., 217, 442.

McCammon, D., Münch, G., and Neugebauer, G. 1967, Ap. J., 147, 575.

Münch, G. and Taylor, K. 1974, Ap. J. (Letters), 192, L93.

Phillips, T. G., Huggins, P. J., Neugebauer, G., and Werner, M. W. 1977, Ap. J. (Letters), 217, L161.

Shull, J. M. 1978, preprint.

Thaddeus, P., Wilson, R. W., Kutner, M., Penzias, A. A., and Jefferts, K. B. 1971, Ap. J. (Letters), 168, L59.

Treffers, R. R., Fink, U., Larson, H. P., and Gautier, T. N. III. 1976, Ap. J., 209, 793.

Turner, J., Kirby-Docken, K., and Dalgarno, A. 1977, Ap. J. Suppl., 35, 281.

Wynn-Williams, C. G., and Becklin, E. E. 1974, Publ. A.S.P., 86, 5.

FIGURE CAPTIONS

Fig. 1 - The Orion Molecular Cloud molecular hydrogen emission as seen in the $v = 1 \rightarrow 0$ S(1) transition with 13" spatial resolution. The crosses indicate the positions of the strong infrared continuum sources. Contour intervals are 6.1×10^{-4} ergs s^{-1} cm^{-2} sr^{-1} so that the contour level labeled 1 is 1.22×10^{-3} ergs s^{-1} cm^{-2} sr^{-1}. The limits of the map are given by the dashed contour for which the signal to noise ratio was five to one.

Fig. 2 - The molecular hydrogen emission in Orion as seen in the $v = 1 \rightarrow 0$ S(1) transition with 5" spatial resolution. Contour intervals are 6.1×10^{-4} ergs s^{-1} cm^{-2} sr^{-1} so that the contour labeled 2 is 2.4×10^{-3} ergs s^{-1} cm^{-2} sr^{-1}. The signal to noise ratio was ten to one for this contour level. The extent of the area mapped is enclosed by the straight line boundary.

Fig. 3 - Data obtained on Pk 1 with 10" resolution for four of the H_2 transitions shown versus wavelength. The dashed lines indicate the chosen continuum baseline levels obtained by averaging the points off the line positions. The error bars represent the statistical uncertainties only. The solid lines are instrumental profiles scaled and fit to the points as an aid to the eye.

Fig. 4 - The plot of $\log N(v,J)/g_j$ vs. E used in deriving the excitation temperatures on Pk 1 and Pk 2 (see §IV(a)).

The uncertainties in log $N(v,J)/g_j$ are calibration and statistical uncertainties; uncertainties in the A values and extinction have not been included. The solid lines are drawn through the v = 1 and 2, J = 3 levels. As discussed in the text the slopes of these lines are inversely proportional to the vibrational excitation temperature.

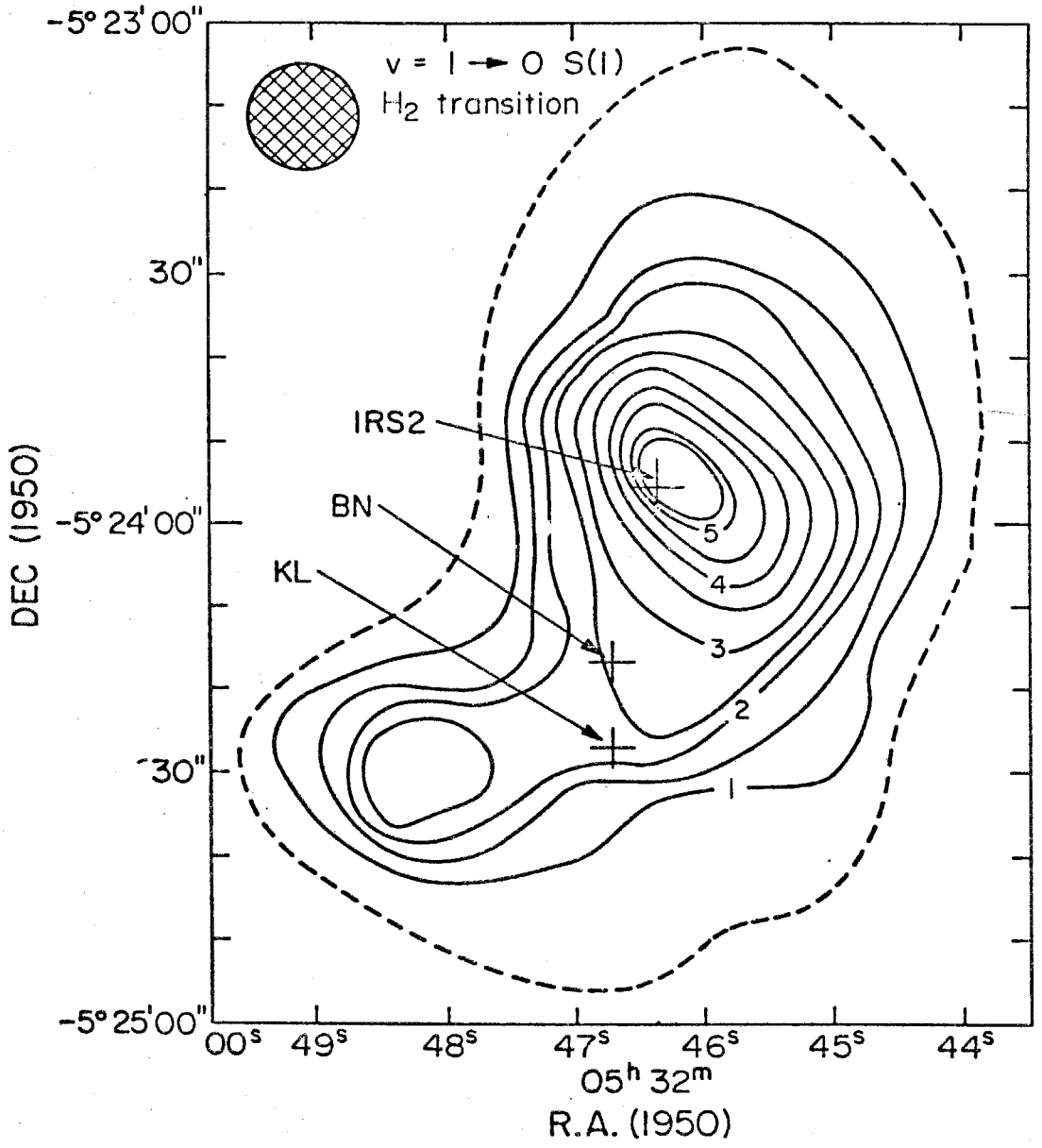
-5° 23' 00"
v = 1 → 0 S(1)
H2 transition
30"
IRS2
BN
KL
-5° 24' 00"
DEC (1950)
5
4
3
2
1
-30"
-5° 25' 00"
00s
49s
48s
47s
46s
45s
44s
05h 32m
R.A. (1950)

Figure 1

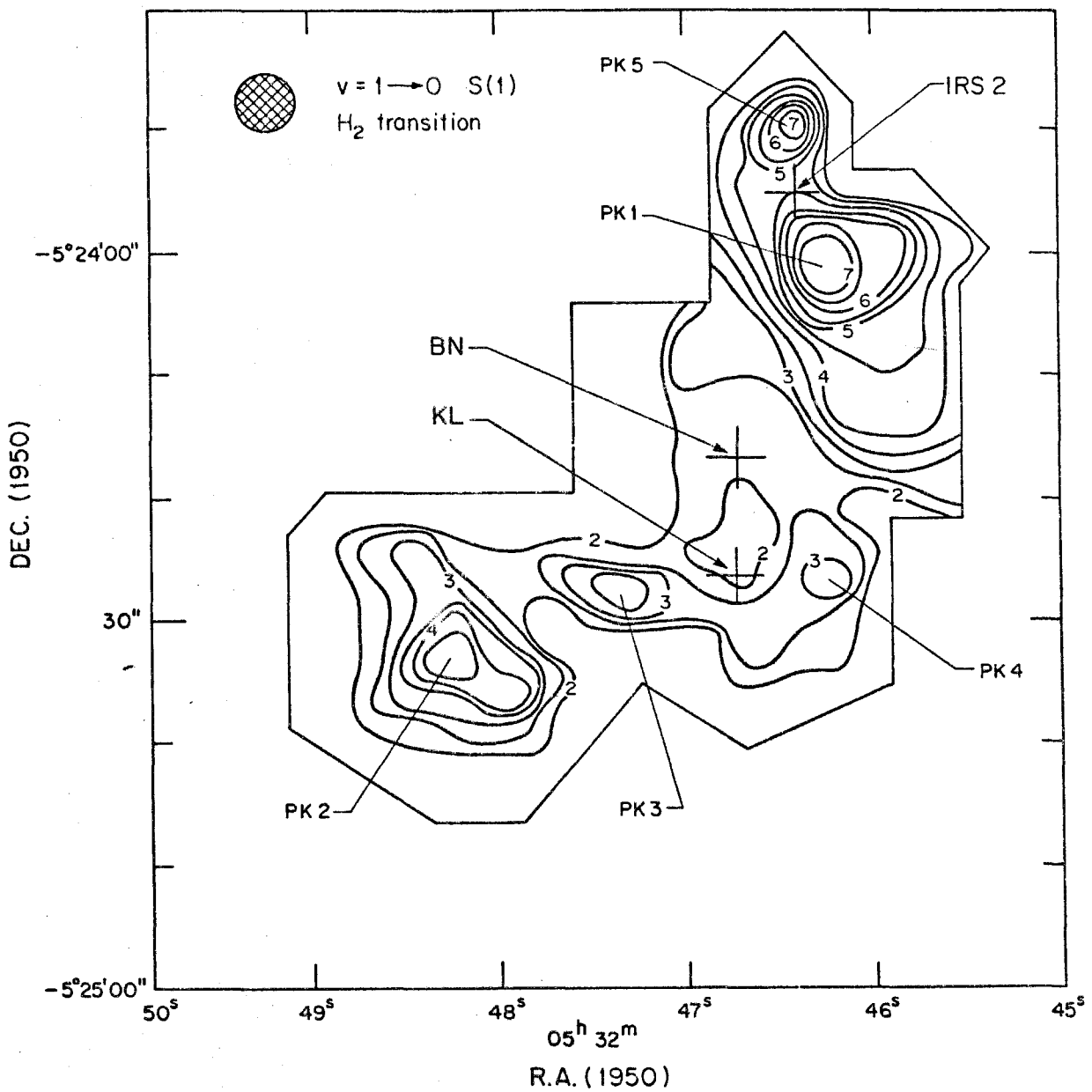
v = 1 → 0 S(1)
H2 transition
PK 5
IRS 2
PK 1
BN
KL
PK 4
PK 2
PK 3
-5°24'00"
30"
-5°25'00"
DEC. (1950)
50s
49s
48s
47s
46s
45s
05h 32m
R.A. (1950)

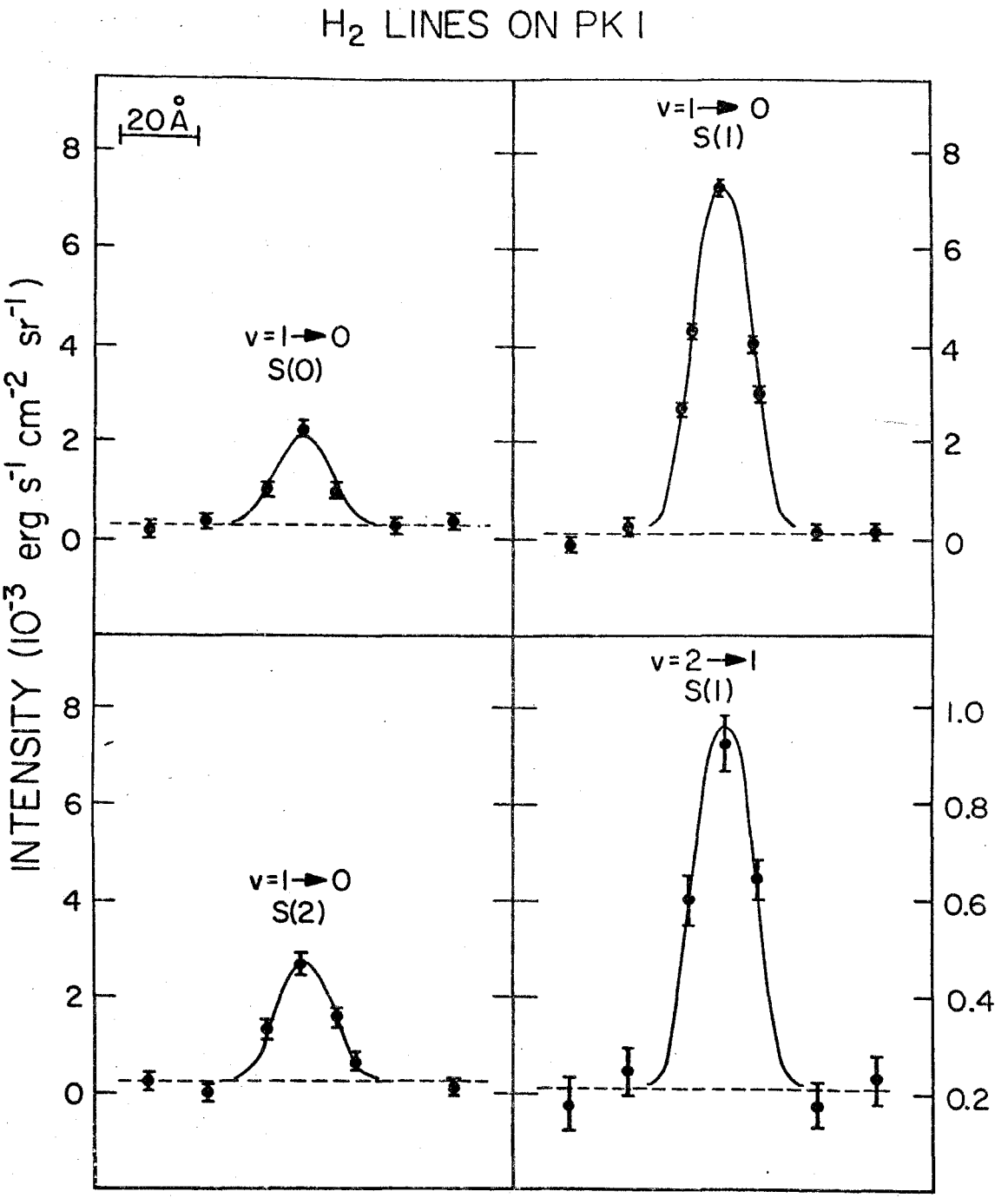
H2 LINES ON PK I
20Å
v=1→0
S(0)
v=1→0
S(1)
v=1→0
S(2)
v=2→1
S(1)
INTENSITY (10-3 erg s-1 cm-2 sr-1)

Figure 3

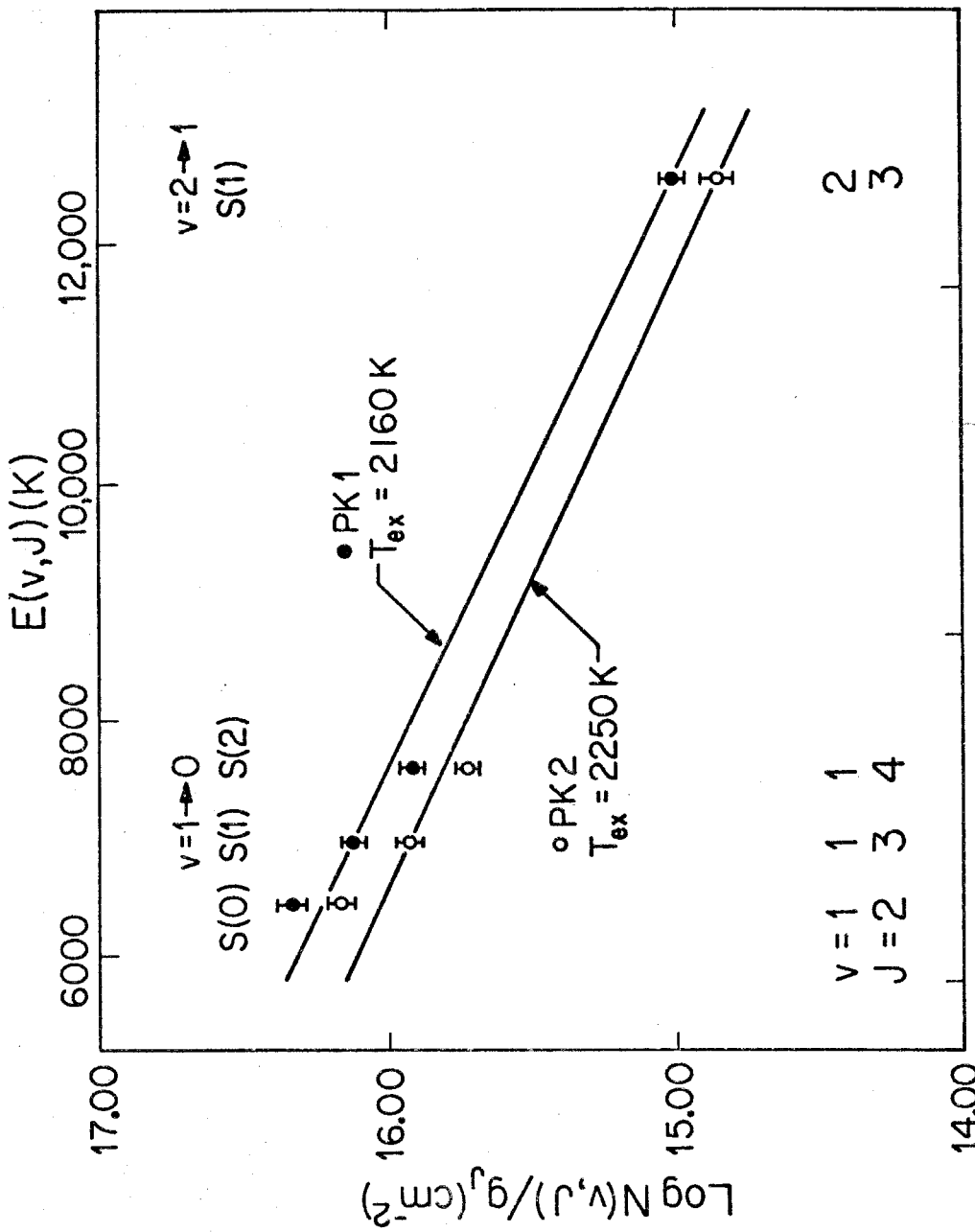
E(v,J)(K)
6000
8000
10,000
12,000
v=1→0
S(0) S(1) S(2)
v=2→1
S(1)
PK 1
T_{ex} = 2160 K
PK 2
T_{ex} = 2250 K
v = 1 1 1
J = 2 3 4
2
3
Log N(v,J)/g_J(cm^{-2})
17.00
16.00
15.00
14.00
0.50
0.75
1.00
E(v,J) (eV)

Figure 4

PAPER 4:

MEASUREMENTS OF THE EXTINCTION TO THE MOLECULAR HYDROGEN EMISSION FROM THE ORION NEBULA

Submitted for publication to

the Astrophysical Journal

in collaboration with

S. E. Persson and G. Neugebauer

I. INTRODUCTION

Observations of the molecular hydrogen emission from Orion have shown the emission region to be a hot ($\sim$ 2000 K) sheet of gas that is approximately 0.1 pc across and centered on the infrared cluster in OMC 1 (Gautier et al. 1976; Grasdalen and Joyce 1976; Beckwith et al. 1978a, hereafter Paper I). The relationship between the emission region and other sources within the molecular cloud is not understood. Although several explanations have been proposed for the origin of this emission none has gained general acceptance.

An important parameter that can be determined observationally is the amount of extinction to the H_2 emission region. A knowledge of the extinction is needed to determine the total H_2 luminosity and to derive line ratios and temperatures. A comparison of the extinction to the H_2 with the extinction estimated to other luminosity sources in the region gives the relative line of sight placement of these sources. This placement is important if the dynamics of the region are to be understood.

In this paper, observations which lead to the extinction to the H_2 emission region are presented. The differential extinction between 2.12 μm and 2.42 μm is derived by observing the intensity ratio of the $v = 1 \rightarrow 0$ Q(3) and S(1) H_2 lines in Orion and comparing this with its unreddened value as measured in NGC 7027. The two lines are optically thin and originate from the same upper level ($v = 1$, $J = 3$) so the intensity ratio is independent of the level population. The

result is checked by a measurement of the intensity ratio of the $v = 1 \rightarrow 0$ Q(4) and S(2) lines which originate from the $v = 1$, $J = 4$ level. Because the density of the molecular cloud OMC 1 is high, the extinction to the H_2 will be large, on the order of a few magnitudes at 2 μm, if the emission region is inside the molecular cloud. Our result should also be compared with the results of Simon et al. (1978) who use the S and O branch lines to measure the reddening.

II. OBSERVATIONS

The observations were made with the 2.2 m telescope at Mauna Kea Observatory using the Ebert-Fastie spectrometer system described in Paper I. The spectral resolution for the observations was ~ 34 Å ($\Delta\lambda/\lambda \sim 1.6 \times 10^{-3}$) and the spatial resolution was 17" FWHM. Sky subtraction was accomplished by chopping 104" in declination.

The observing technique was similar to that used to determine the line ratios in Paper I. For each measured line at each position on the sky, the intensity at several wavelengths was measured and fit with an instrumental profile to determine the wavelength of the line center. The line intensities were then found by measuring three points of the spectrum, one at the line wavelength and one on each side of the line wavelength to establish the continuum baseline. The repeatability of the wavelength calibration was checked using a laboratory argon lamp.

Measurements were made at three different positions in Orion shown in Figure 1. The average surface brightnesses of the $v = 1 \rightarrow 0$ S(1) line into a 17" aperture are 5.7 ± 0.9, 3.2 ± 0.5, and 1.5 ± 0.2

(10^{-3} ergs s^{-1} cm^{-2} sr^{-1}) at positions 1, 2 and 3 respectively. The two lines of interest were always measured alternately and in rapid succession, so that the uncertainties caused by variations in the seeing, guiding, and atmospheric transmission were minimized in the ratio. The different spatial points were measured differentially with respect to the brightest point, Position 1.

Atmospheric absorption bands due to water vapor around 2.4 μm and 2.0 μm potentially cause large systematic uncertainties in the measurement of the Q(3), Q(4), and S(2) lines. The atmospheric water vapor content at Mauna Kea Observatory is typically very low, however, and telluric absorption near 2.4 μm is minimized. In order to check the extent to which the atmosphere affected the measured line ratios, the line strengths from Position 1 were measured over an airmass range of roughly 1.1 to 2.1 each night. At Position 1, the line strengths so dominate the underlying continuum that the measured airmass correction applies to the line itself and not to the continuum. The resulting airmass corrections were all negligible. Airmass corrections for the continua were determined by measuring the star ε Ori over a large airmass range. No airmass corrections to the line ratios greater than 0.03 mag per airmass were found. ε Ori was measured at all of the line wavelengths and several adjacent wavelengths described in section IIb. The adjacent wavelengths were chosen to contain no saturated telluric absorption features and a minimal number of weak telluric features as determined from the spectra of Hall (1974).

The measured line ratios in Orion will each be the product of three parts. The first part is the intrinsic ratio of line intensities

that is emitted at the source. The second part is the change in the intensity ratio which results from reddening. The third part is the relative system response at the two different wavelengths. In order to determine the reddening, it is necessary to know the product of the first and third factors, that is the ratio that would be observed from an unreddened, celestial, molecular hydrogen source. This product has been determined in two independent ways as described below.

a) Measurement of NGC 7027

The use of a celestial molecular hydrogen line source to calibrate the system response is useful because it minimizes several uncertainties in the calibration procedure. NGC 7027 has a relatively small visual extinction (Miller and Mathews 1972) and so the differential extinction between 2.12 μm and 2.42 μm is negligible. We assume therefore that a measurement of Q(3)/S(1) intensity ratio in NGC 7027 is a measurement of the unreddened Q(3)/S(1) intensity ratio.

The relative system response at the two wavelengths affects the measurements of Orion and NGC 7027 in the same way. In particular, the response to line radiation is measured directly; the effective bandwidth of the spectrometer does not enter into the calibration. Additionally, the size of the H_2 emission region in NGC 7027 is $\sim$ 10" (Beckwith et al. 1978b), comparable to the size of the emitting region at Position 1. If there is a difference in the system response to pointlike and extended sources then measurements of NGC 7027 and Orion will be affected in the same way. Furthermore, uncertainties in

the theoretical intensity ratio of the Q(3)/S(1) lines do not enter in to the derived reddening. Thus a comparison of the ratio as measured in these sources gives a reliable estimate of the reddening to Orion.

b) Measurement of ε Ori

A second procedure used to find the system response to the unreddened Q(3)/S(1) ratio was to measure ε Ori (BOI) between 2.0 μm and 2.5 μm. Because the Q(4) and S(2) lines are faint and could be measured in NGC 7027 only with large statistical uncertainties the unreddened Q(4)/S(2) ratio in Orion was calibrated using this procedure only. This procedure is subject to greater uncertainties than that based on NGC 7027 since it involves corrections for bandwidth, beam profile variations, and atmospheric absorption at each wavelength.

The intensity response of the system was derived from each stellar measurement by assuming that

$$I = R\, F_\lambda\, \Delta\lambda\, 10^{-A\eta}$$

where R is the system response, F_λ is the stellar flux, $\Delta\lambda$ is the bandwidth, A is the airmass correction, η is the airmass, and I is the measured intensity; all of these parameters are functions of wavelength. F_λ was assumed to follow the Rayleigh-Jeans law between 2.0 μm and 2.5 μm while $\Delta\lambda$ was determined from measurements of the instrumental profile of laboratory source lines at several wavelengths.

In order to minimize the effects of telluric absorption in the stellar flux measurements at the longer wavelengths, measurements were made at 2.4016 μm, 2.4290 μm, and 2.4394 μm. These wavelengths

are close to the wavelengths of the Q(3) and Q(4) lines and contain only a small number of weak telluric features. It was assumed that the system response was a smooth function of wavelength; the stellar intensities at the H_2 line wavelengths were derived from the measured intensities at the selected wavelengths by interpolation. The airmass corrections applied to the selected wavelengths were all less than 0.03 mag per airmass.

After the system response was derived from the stellar observations, the unreddened intensity ratios were determined from this and the theoretical intensity ratio for each pair of lines. The theoretical ratios were calculated using the frequencies measured by Fink, Wiggins, and Rank (1965); and the Einstein A coefficients of Karl and Poll (1966) except for the Q(4) line. For the Q(4) line, the Einstein A coefficient of Turner, Kirby-Docken, and Dalgarno (1977) was used.

The uncertainty in this process was estimated by assigning a 5% uncertainty to the calculated bandwidth, a 5% uncertainty to the photometric measurements which includes the uncertainty in the assumption of a Rayleigh-Jeans continuum and the uncertainty in the derived airmass corrections, a 5% uncertainty in the beam profiles, and a 10% uncertainty in the Q(4) Einstein A coefficient of the line. The third uncertainty comes about because the calibration stars are unresolved but the line emission regions in Orion are resolved and there may be a difference in the overall response at the different wavelengths. The overall uncertainty is thus 9% for Q(3)/S(1) and 15% for Q(4)/S(2).

III. RESULTS

The results of the line ratio measurements are shown in Figure 2 for the line pairs Q(3)/S(1) and Q(4)/S(2) respectively. The main result of this work is that there is significant reddening between 2.12 μm and 2.42 μm to the molecular hydrogen emission in Orion. The measured Q(3)/S(1) intensity ratio in Orion is substantially greater than in NGC 7027; the direct comparison implies 0.9 ± 0.2 mag of reddening between 2.12 μm and 2.42 μm. If the measured ratio in Orion is compared to the expected ratio for no reddening based on measurements of ε Ori, the differential extinction is 0.6 ± 0.2 mag. A comparison of the Q(4)/S(2) intensity ratio in Orion with the calculated ratio for no reddening gives a differential extinction between 2.03 μm and 2.43 μm of 0.7 ± 0.2 mag. Thus three independent measurements imply that the extinction to the region of H_2 emission in Orion is of order 0.8 mag between 2.12 μm and 2.42 μm.

A second result indicated by Figure 1 is that the differential extinction is not significantly different at the three places measured. As indicated above, the intensity of the S(1) line is variable from position to position. If surface brightness variations in the H_2 emission were due solely to variations in the intervening extinction then a larger change in the measured ratio would be expected than is seen. It can therefore be concluded that the observed variations in surface brightness of H_2 emission do not result solely from variations in the intervening extinction to the source.

The total infrared and optical extinction to the emission region can be inferred from the above results. If the extinction is a smooth function of wavelength between 2.0 μm and 2.4 μm and the extinction law is given by van de Hulst's curve #15 (van de Hulst 1946, Johnson 1968) then there are 5.0 mag of extinction at 2.12 μm and 50 mag of visual extinction for 1 mag of differential extinction between 2.12 μm and 2.42 μm. For Position 1, if the differential extinction is taken to be 0.9 ± 0.2 mag the 2.1 μm extinction is 4.5 ± 1 mag and the visual extinction is 45 ± 10 mag.

These results can be used to correct the results of previous measurements of the H_2 emission lines in Orion (Paper I). All the measured line strengths will be increased by about a factor of fifty to give the true line strengths. This means that the total H_2 luminosity and derived column densities are approximately two orders of magnitude greater than concluded on the basis of the uncorrected line intensities. The total H_2 luminosity is $\sim$ 3000 $L_\odot$ and the average column density is $\sim 5 \times 10^{20}$ cm^{-2}.

The absolute line intensities are subject to considerable uncertainty, because they depend on applicability of the assumed extinction law. The corrected line ratios, however, are primarily subject to the uncertainty in the estimated slope of the extinction curve. Thus the rotational and vibrational temperatures can be corrected with some confidence.

Figure 3 shows the logarithm of normalized column density of vibrational excited H_2 molecules versus the energy of the excited state. This figure is similar to Figure 4 of Paper I but with N (v,J)

corrected for extinction. As discussed in Paper I, the temperature depends only on the column density ratios and is inversely proportional to the slope of a line connecting the states.

It is seen from Figure 3 that, within the uncertainties, there is no difference between the derived rotational and vibrational temperatures. This result supports the assumption that the molecules are collisionally excited and in thermal equilibrium with their surroundings. The derived temperature is $\sim$ 2000 K.

IV. DISCUSSION

The implication of these results is that the region of molecular hydrogen emission in Orion lies within the molecular cloud. The visual extinction to the H II region and the Trapezium stars is small and so the emission region lies some distance behind these sources. Although the distance into the cloud cannot be estimated accurately, it is of interest to compare the extinction to the H_2 with that estimated to other sources in Orion. On the basis of the 10 μm absorption feature, Gillett et al. (1975) estimate the visual extinction to the BN source to be $\sim$ 50 magnitudes. This is comparable to the extinction we have derived to the H_2 emission. In contrast to this, the visual extinction through the entire molecular cloud is estimated by Thaddeus et al. (1971) to be $\sim$ 200 magnitudes. These estimates place the molecular hydrogen emission quite close to the infrared cluster and within the molecular cloud.

Both the depth of the emission region into the cloud and the revised energy requirements place constraints on the way in which the H_2 can be vibrationally excited. In particular, no source outside of the molecular cloud can excite the H_2 molecules radiatively. Furthermore, since radiative excitation occurs at ultraviolet wavelengths where the dust absorption cross section is relatively large it is unlikely that a single source inside the cloud can pump the H_2 molecules. At the high densities within the cloud ($\gtrsim 10^5$ cm^{-3} Thaddeus et al. 1971; Liszt et al. 1974; Evans et al. 1975) the extinction at 1000 Å between any such source and the outer portions of the region of H_2 emission is prohibitively large.

The second main result of the extinction measurements is that the amount of energy involved in keeping the H_2 excited is of order fifty times larger than indicated by earlier line intensity measurements. The derived luminosity, inferred column densities, and power requirements are increased in direct proportion to the measured extinction. If the emission region is shock heated (Hollenbach and Shull 1977, London, McCray, and Chu 1977; Kwan 1977), the increase requires the derived minimum preshock molecular density to be $\sim 10^7$ cm^{-3}. This density is quite high and applies to an area at least as large as that over which H_2 emission is seen $\sim$ (0.2 pc)^2. The conclusion that such a shock cannot be driven continuously by any objects observed in Orion (Hollenbach and Shull 1977; Kwan 1977; Paper I) is greatly strengthened. In particular, radiation pressure or stellar winds from any of the known luminosity sources in OMC 1 cannot provide the energy necessary to keep the shock moving through such a dense medium.

Finally, the fact that the placement of the emission region within the cloud agrees generally with that inferred for the infrared cluster implies that the two are related. Although we propose no causal connection here, the combination of this coincidence with the number of other observations which show this region to be the site of some peculiar energetic phenomena (Zuckerman, Kuiper, Rodriguez-Kuiper 1976; Kwan and Scoville 1976; Genzel and Downes 1977) is suggestive. If the H_2 emission is the result of some event which is related to the infrared cluster then an understanding of the H_2 energetics should yield valuable clues to both the dynamics of this region.

SUMMARY

From the measurement of the Q(3)/S(1) intensity ratio in Orion the following results are obtained:

(1) The differential extinction between 2.12 μm and 2.42. μm is 0.9 ± 0.2 mag. This result implies a 2.1 μm extinction of 4.5 ± 1 mag and a visual extinction of 45 ± 10 mag.

(2) The vibrational and rotational temperatures derived from the line intensities corrected for reddening are equal to within the uncertainties. The result is 2000 K.

(3) The emission region lies within the molecular cloud, probably at the same depth as the infrared cluster.

(4) The column densities and power requirements for H_2 excitation are of order fifty times larger than concluded from line intensity measurements alone.

REFERENCES

Beckwith, S., Persson, S. E., Neugebauer, G., and Becklin, E. E. 1978a (Paper I), Ap. J., in press.

Beckwith, S., Becklin, E. E., Neugebauer, G., and Matthews, K. 1978b, in preparation.

Evans, N. J. II, Zuckerman, B., Sato, T., and Morris, G. 1975, Ap. J., 199, 383.

Fink, U., Wiggins, T. A., and Rank, D. H. 1965, J. Molec. Spectrosc., 18, 384.

Gautier, T. N. III, Fink, U., Treffers, R. P.,and Larson, H. P. 1976, Ap. J. (Letters), 207, L129.

Genzel, R., and Downes, D. 1977, Astr. and Ap., 61, 117.

Gillett, F. C., Forrest, W. J., Merrill, K. M., Capps, R. W., and Soifer, B. T. 1975, Ap. J., 200, 609.

Grasdalen, G. L., and Joyce, R. R. 1976, Bull. A.A.S., 8, 349.

Hall, D.N.B. 1974, An Atlas of Infrared Spectra of the Solar Photosphere and of Sunspot Umbrae, (Tucson: Kitt Peak National Observatory).

Hollenbach, D. J., and Shull, J. M. 1977, Ap. J., 216, 419.

Johnson, H. L. 1968, in Nebulae and Interstellar Matter, eds. B. M. Middlehurst and L. H. Aller (Chicago: University of Chicago Press), p. 167.

Karl, G., and Poll, J. D. 1967, J. Chem. Phys., 46, 2944.

Kwan, J. 1977, Ap. J., 216, 713.

Kwan, J., and Scoville, N. 1976, Ap. J. (Letters), 210, L39.

Liszt, H. S., Wilson, R. W., Penzias, A. A., Jefferts, K. B., Wannier, P. G., and Solomon, P. M. 1974, Ap. J., 190, 557.

London, R., McCray, R., and Chu, S. I. 1977, Ap. J., 217, 442.

Miller, J. S., and Mathews, W. G. 1972, Ap. J., 172, 593.

Simon, T., Simon, M., Joyce, R., and Righini-Cohen, G. 1978, in preparation.

Thaddeus, P., Wilson, R. W., Kutner, M., Penzias, A. A., and Jefferts, K. B. 1971, Ap. J. (Letters), 168, L59.

Turner, J., Kirby-Docken, K., and Dalgarno, A. 1977, Ap. J. Suppl., 35, 281.

van de Hulst, H. C. 1946, Recherches Astronomiques de l'Obs. d'Utrecht, 11, part 1.

Zuckerman, B., Kuiper, T.B.H., and Rodriguez-Kuiper, E. N. 1976, Ap. J. (Letters), 209, L137.

FIGURE CAPTIONS

Fig. 1 - The positions of the line ratio measurements shown on a map of the H_2 emission made with 13" resolution (Paper I). The circles correspond to an aperture diameter of 17" FWHM and the labels are those used in Figure 2 and the text.

Fig. 2 - Measurements of the H_2 line ratios Q(3)/S(1) and Q(4)/S(2) at the positions shown in Figure 1. The abscissa represents independent measurements of the ratio. The ordinate scale gives the intensity ratio uncorrected for the instrumental response. The partially dashed lines give the ($\pm$ 1σ) limits of the instrumental response to the intensity ratio assuming no reddening. The zero has been set equal to the measured ratio on NGC 7027. The sense of the variations is such that as the lines are reddened the intensity ratio should increase.

Fig. 3 - The normalized column densities of molecules in the state (v,J) are plotted versus the energy of that state above the ground state. Here N' (v,J) is the column density of molecules in the (v,J) state corrected for extinction, g_J is the statistical weight of the state, E(v,J) is the energy of the state above the ground state. The uncertainties in the points do not include uncertainties in the reddening corrections which may be large. The plotted uncertainties for the v = 1 levels result from calibration uncertainties in the original data so that deviations from the assumed linear relationship that result will be correlated between Pk 1 and Pk 2.

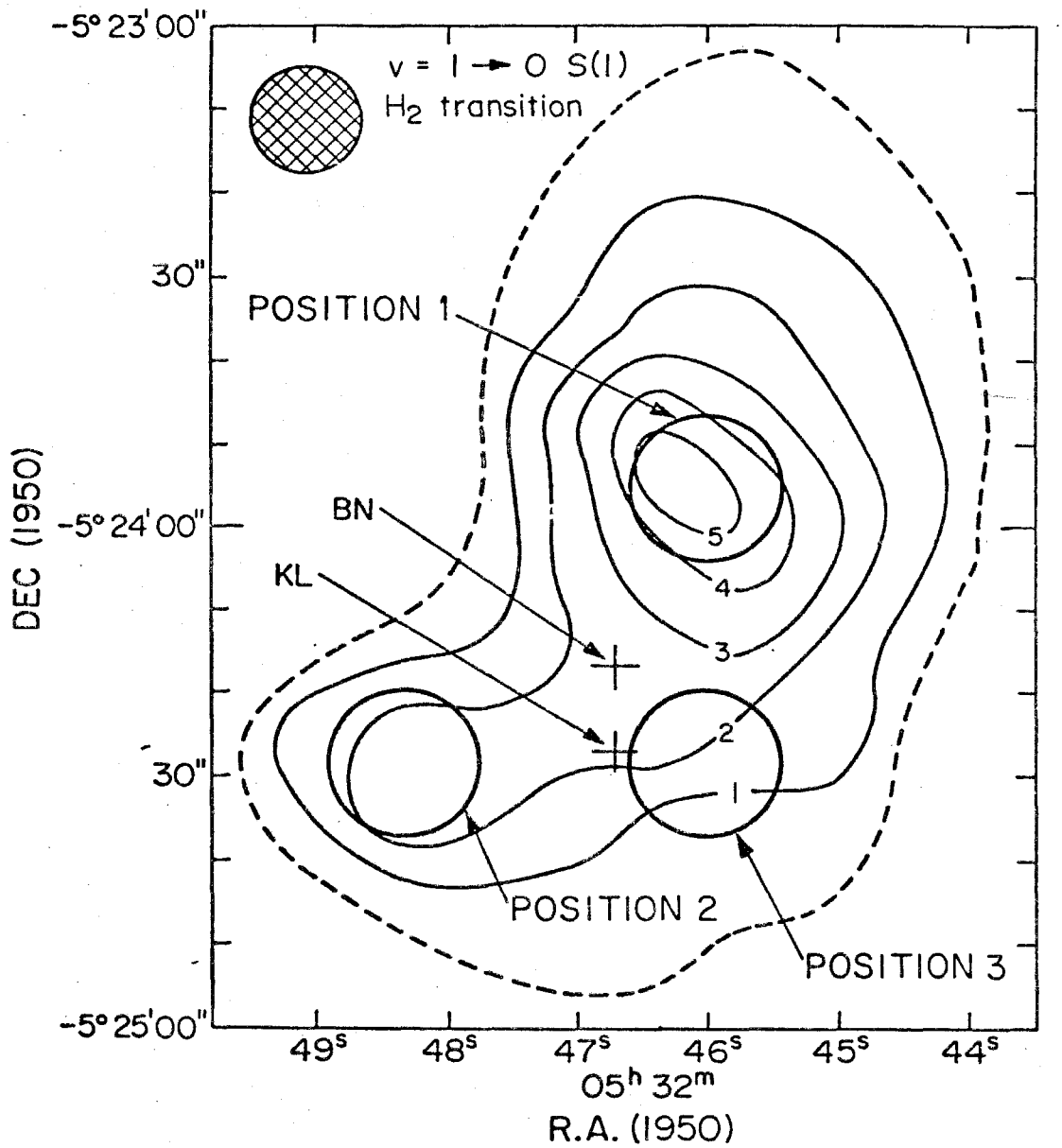
-5° 23' 00"
v = 1 → 0 S(1)
H2 transition
30"
POSITION 1
BN
KL
5
4
3
2
1
-5° 24' 00"
30"
POSITION 2
POSITION 3
-5° 25' 00"
DEC (1950)
49s
48s
47s
46s
45s
44s
05h 32m
R.A. (1950)

Figure 1

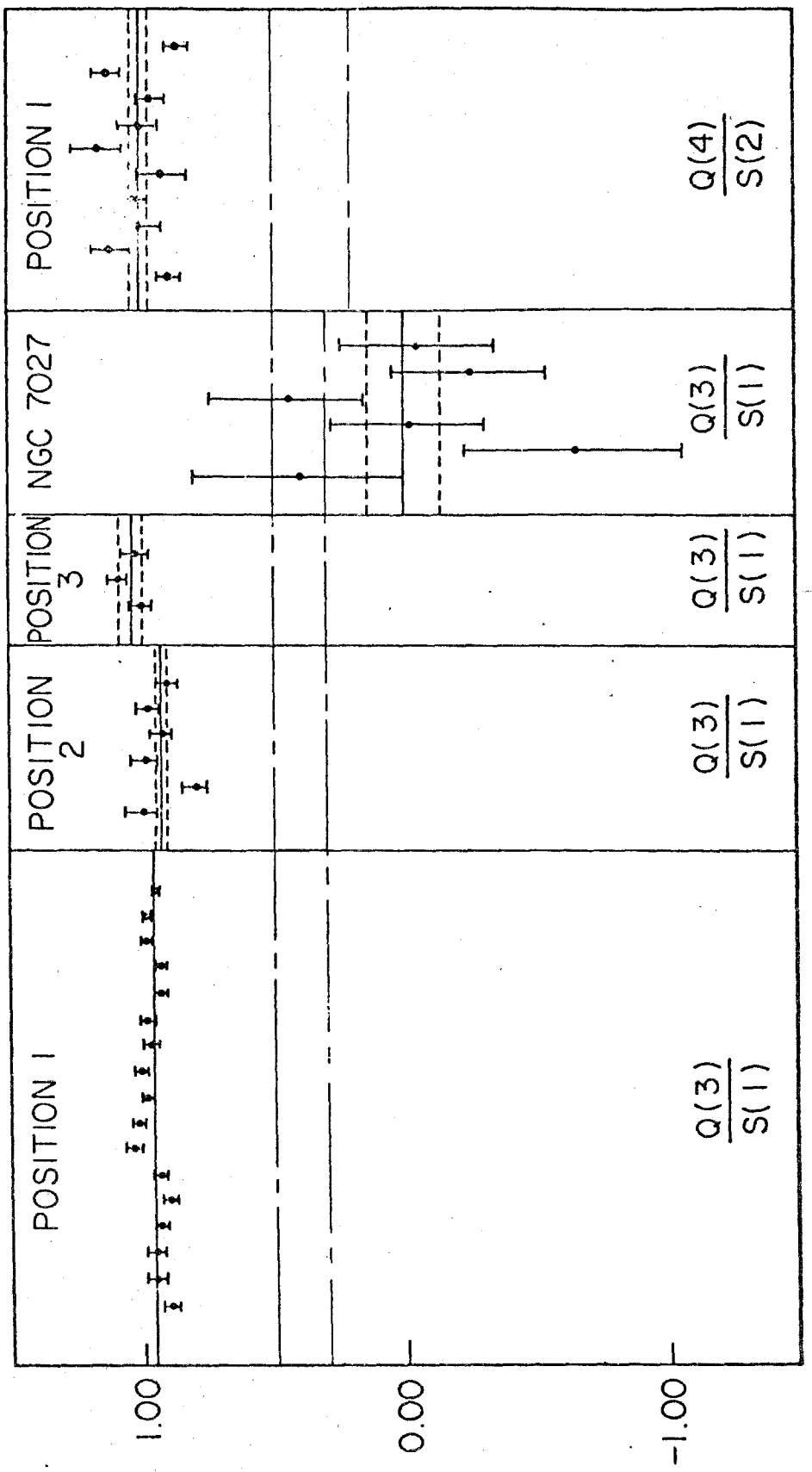
POSITION 1
POSITION 2
POSITION 3
NGC 7027
POSITION 1
Q(3)/S(1)
Q(3)/S(1)
Q(3)/S(1)
Q(3)/S(1)
Q(4)/S(2)
1.00
0.00
-1.00
2.5 LOG (RATIO)

Figure 2

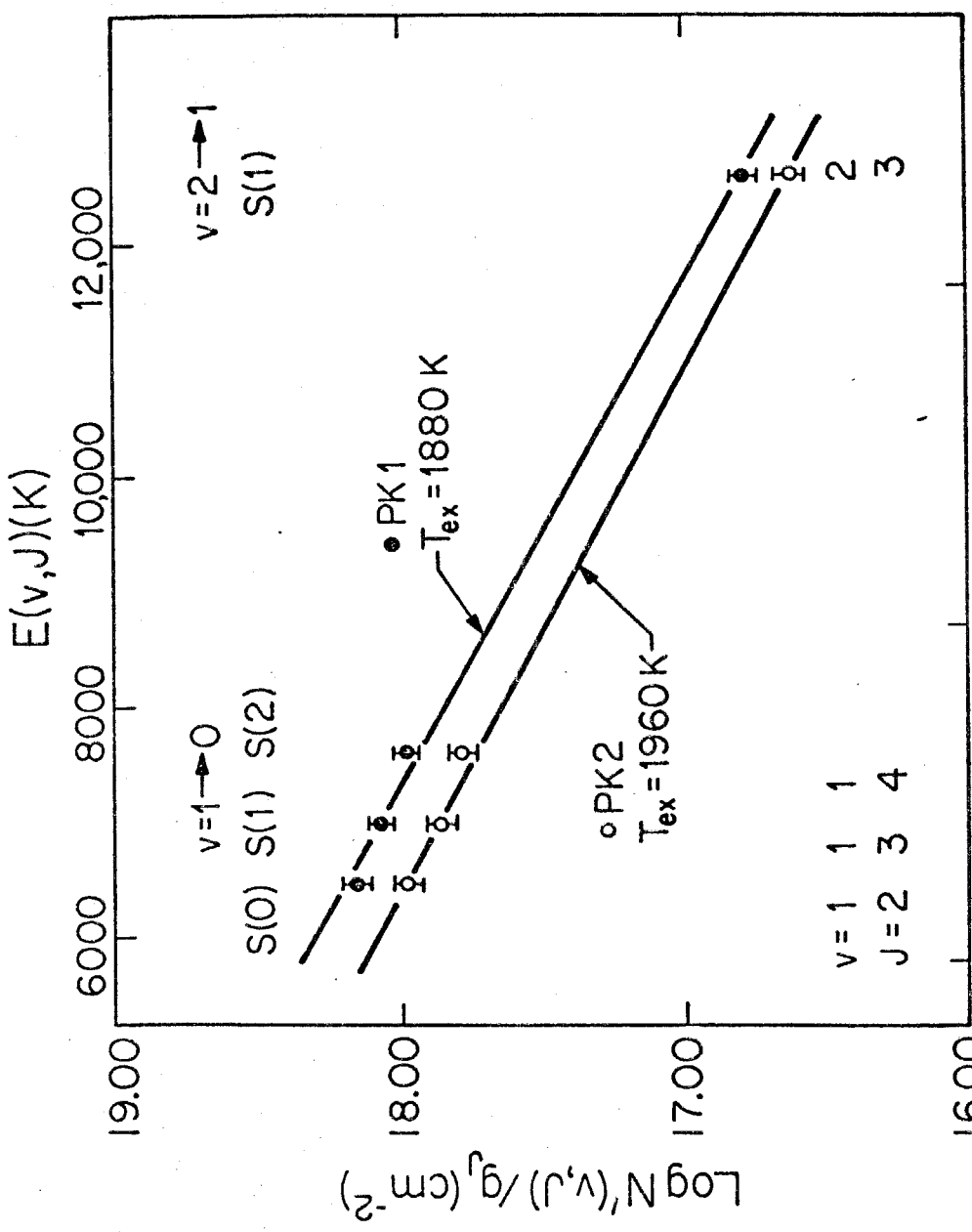
E(v,J)(K)
6000
8000
10,000
12,000
E(v,J)(eV)
0.50
0.75
1.00
Log N'(v,J) /g_J (cm^-2)
19.00
18.00
17.00
16.00
v=1→0
S(0) S(1) S(2)
v=2→1
S(1)
PK1
T_ex = 1880 K
PK2
T_ex = 1960 K
v = 1 1 1
J = 2 3 4
2
3

Figure 3

SUMMARY

The discovery of molecular hydrogen emission from the Orion nebula by Gautier, et al. (1976) and from NGC 7027 by Treffers et al. (1976) was particularly fortuitous because, although many suggestions had been made to observe H_2, no one had anticipated the intense emission observed from these two objects. Of all the theories of H_2 excitation put forth before these discoveries, none could adequately explain either the strength of the emission or the relative intensities of the several observed emission lines. These discoveries created an immediate interest in the observation of vibrationally excited molecular hydrogen. The existence of an unanticipated mechanism to excite the molecule might allow widespread observations of its abundance and distribution in interstellar clouds.

When the work for this thesis began, we believed that the discovery and study of new sources of molecular hydrogen emission would help us to understand the circumstances which give rise to this emission in the known sources. An accurate picture of the physical conditions within the emission range might help us to predict H_2 emission in new objects and indicate how we might observe the majority of the H_2 in the interstellar medium. Because molecular hydrogen has a large number of observable transitions at infrared wavelengths, these observations would motivate further advances and give astronomers a new tool for the study of interstellar gas.

We approached the problem in two ways. First, we searched a variety of objects for new sources of H_2 emission. The new sources

would provide a sample to serve as a basis for further study. By comparing the overall properties of the objects which exhibit H_2 emission, we hoped to isolate those properties necessary for the excitation of H_2. For the bright or nearby sources, a variety of additional observations could be made to probe the physical conditions within each source. Second, we made a number of observations of the brightest source, the Orion nebula, furthering the work started by Gautier et al. (1976) and Grasdalen and Joyce (1976). These observations were intended to probe the conditions within Orion and to understand the nature of the observed H_2.

The following discussion describes the results of this work and the conclusions which result from an analysis of Orion and seven new sources of molecular hydrogen emission. Separate sections have been written for the results of the search and the study of Orion. The conclusion which results from the analysis presented in these sections is that the hydrogen in all the observed sources is excited by strong shock waves. This excitation mechanism was not entirely unanticipated in the last decade but its overall importance had been largely overlooked until two years ago.

I. SEARCH FOR H_2 EMISSION

The results of the search for molecular hydrogen emission are presented in the table on page 4 of this thesis. The objects in the table were chosen because they exhibit a range of physical properties.

In the selection of objects for this survey, we were guided by three crude ideas. First, since the excitation temperature of the upper level of the line in which the search was made ($v = 1 \rightarrow 0$ S(1)) is of order 7000 K, we included objects with regions of gas at temperatures greater than 1000 K, or with ultraviolet luminosity sources which might pump the molecules in the ultraviolet absorption bands (see section Ia). HII regions, planetary nebulae, T Tauri stars, and supernova remnants are examples of these objects. Second, we included objects thought to be similar to the Orion nebula and NGC 7027; the table contains a number of dense molecular clouds with embedded infrared clusters and a variety of young, high density planetaries. Third, since the detection of H_2 emission from an object might reveal new facts about the physical conditions within the object, we included a number of objects of general astronomical interest such as Sgr A, M 82, and IRC +10216.

We will use the results of the survey to understand the way in which molecular hydrogen is vibrationally excited in the new emission sources. The best available theories of H_2 excitation, when applied to the observational results, show that the observed H_2 emission probably originates in the heated transition layers of strong shock waves. This conclusion is strengthened by comparing the properties of the new H_2 emission sources with the properties of the objects which do not show H_2 emission. Neither the theory nor the observations unequivocally determine the excitation process for the molecular hydrogen. It will be shown, however, that all of the evidence supports

the same hypothesis

a) Theory

It was realized over twenty years ago that molecular hydrogen might play an important role in the development of the interstellar medium and many possible ways of observing the molecule were discussed. Much of this discussion centered on processes which could excite H_2 into its many rotational and vibrational states. One of the earliest (see Gould and Harwit 1963) and best theories suggested that molecular hydrogen is excited through the resonant absorption of ultraviolet light (1000 Å) in the molecular electronic bands and that it subsequently decays to excited vibrational levels of the ground electronic bands. Black and Dalgarno (1976) and Shull (1978) have made detailed calculations of the relative near infrared line intensities which result from this process. Field et al. (1968), Aannestad (1973), and a number of other authors (Hollenbach and Shull 1977; Kwan 1977; London, McCray, and Chu 1977) discussed collisional excitation of H_2 in the discontinuity behind a strong shock wave. The most recent calculations have been made specifically to explain the intense H_2 emission from the Orion nebula. Black (1978) suggested that H_2 may be excited by electron collisions in the boundary layers between regions of ionized gas and regions of neutral material, although he notes the cross sections are probably too small to excite detectable numbers of molecules. Spitzer and Cochran (1973) suggested that after

forming on dust grains H_2 molecules are ejected in excited vibrational states (see also Hollenbach and Salpeter 1971) and we might observe the subsequent radiative decays. By using the H_2 formation rates of Hollenbach, Werner, and Salpeter (1971), their result that the fractional abundance of molecular hydrogen is essentially unity one visual optical depth into the cloud, an H_2 volume density of 10^4 cm^{-3}, and the optimistic assumption that one $v = 1 \rightarrow 0$ S(1) photon is emitted for every formation, we find that expected emission intensity is at least an order of magnitude less than the best limits in the table. Of all the possible ways suggested to produce excited moleucles, only ultraviolet pumping and collisional excitation in shock waves appear likely to produce detectable column densities of vibrationally excited H_2.

Assuming ultraviolet excitation of a model cloud, Black and Dalgarno (1976) predict H_2 emission intensities two orders of magnitude less than the best upper limits in the table. Shull (1978) has recalculated the emission line intensities from a different model. He concludes that dust absorption, saturation of the ultraviolet absorption lines, and multiple absorptions from excited vibrational states limit the column densities of molecular hydrogen in the $v = 1$ state to less than 2×10^{16} cm^{-2}; he requires H_2 volume densities greater than or equal to 10^5 cm^{-3} to achieve this column density. These densities are somewhat higher than those expected in most of

the new H_2 emission sources. Shull notes that his calculation does not include the effects of near resonant collisions, principally because accurate cross sections are not known. These collisions can redistribute the level populations and enhance the population of the v = 1 state. The cross sections for inelastic collisions between vibrationally excited molecules and ground state molecules (which greatly outnumber excited molecules) become large when the sum of internal energies of the incident molecules is within kT (the average thermal energy) of the sum of internal energies of the post collisional molecules. For example, the cross section for the reaction $H_2(v = 2) + H_2(v = 0) \rightarrow H_2(v = 1) + H_2(v = 1)$ is considerably larger than the normal inelastic cross sections when the stated energy condition is met. Thus, the column density of molecules in the v = 1 state may be significantly larger than Shull's prediction as a result of these collisions and we must regard his results with caution. He notes, however, that the uncertainty introduced by the neglect of these collisions is, at most, a factor of eight in the level populations.

If we use Shull's column density limit of 10^{16} cm^{-2} and generously assume that 20% of these molecules are in the J = 3 states, then the upper limit to the intensity of emission in the $v = 1 \rightarrow 0$ S(1) transition is 10^{-4} ergs s^{-1} cm^{-2} sr^{-1}. This intensity is smaller than the measured intensities of all but one of the new emission line sources in the table. The measured intensities are, in some cases, lower limits since the emission line regions may not

be spatially resolved (compare, for example, the intensities measured from CRL 618 with 5" and 10" apertures). Even making optimistic assumptions about the volume densities and level populations, we cannot easily explain the observed H_2 emission intensities by assuming they are radiatively pumped. Additionally, the upper limits in the table do not place any useful restrictions on the physical parameters of the objects which do not exhibit H_2 emission since these upper limits are greater than 10^{-4} ergs s^{-1} cm^{-2} sr^{-1} in almost all cases.

For the case of shock excitation, the calculations of Hollenbach and Shull (1977), Kwan (1977), and London, McCray, and Chu (1977) require strong shocks to produce the observed line strengths in any of the objects. The necessary H_2 volume densities are, however, considerably less than those required by the ultraviolet pumping theory. Kwan shows that a 10 to 20 km s^{-1} shock wave in a gas with an H_2 volume density of order 10^4 cm^{-3} will produce an H_2 intensity in the $v = 1 \rightarrow 0$ S(1) transition of 10^{-4} ergs s^{-1} cm^{-2} sr^{-1}. This density is comparable to other measured densities in many of the new emission sources (e.g., the electron density) and it is reasonable to believe that these sources contain regions of H_2 with hydrogen densities of this order. Furthermore, there is no upper limit to the intensity of H_2 emission that can be produced by shock waves, at least up to 10^{-2} ergs s^{-1} cm^{-2} sr^{-1}, and emission results from a range of shock velocities (see section IIc). Strong shock waves can easily produce the emission intensities of every source in the table.

On the other hand, since the model requires relatively energetic shock waves to produce observable H_2 emission, the upper limits in the table place no useful constraints on physical conditions within the observed objects. The analysis of Orion, presented later in this summary, is illustrative of this point. In Orion, the H_2 is likely to be shock heated but we must postulate an unusually strong, unobserved energy source to explain the shock. The H_2 emission from Orion could not have been confidently predicted from previous observations. Similarly, it is not possible to quantitatively predict H_2 emission from any of the objects in the table. The upper limits we present are most useful as a guide to future observers.

The application of the best available theoretical calculations to the new molecular hydrogen emission sources shows that the strength of the observed emission is relatively easy to account for by assuming shock excitation of the H_2. The measured intensities are too large to be easily accounted for assuming excitation through the absorption of ultraviolet radiation.

b) Interpretation of the Table

The comparison of the objects which exhibit H_2 emission with those which do not is severely hampered by the small range of observed emission line intensities. This problem is particularly evident among the planetary nebulae and results mainly from inadequate sensitivity. For example, the measured H_2 intensities from NGC 2440 and Hb 12 are at or below the limits that were set on H_2

emission from NGC 6543 and VV 8. The limits are variable because the sensitivity of the experiment varies with aperture size and time spent on each object, and because the sensitivity improved as the system was modified. In addition, some objects are quite extended so the time spent at each spatial position was reduced to allow the sampling of a large area. This lack of uniformity poses a particular problem because many of the new emission sources have H_2 line intensities equal to or less than the limits set on the other objects.

Because the range of the detected intensities is small, and close to the best upper limits in the table, the uncertainty in the extinction to many of the objects also makes these comparisons difficult. For example, the limit of H_2 emission from NGC 7538 IRS 2 is quite good compared with most of the other objects in the sample. However, the visual extinction to this object is estimated to be 20 mag by Willner (1976) which corresponds to 2 mag at the wavelength of the H_2 line. To account for this extinction, the limit shown in the table should be raised by a factor of six. The extinction uncertainty especially affects the comparison of planetary nebulae and H II regions. The extinction to a typical planetary nebula is relatively small (Cahn and Kaler 1971) whereas many of the HII regions are heavily obscured (Wynn-Williams and Becklin 1974).

In spite of the difficulties discussed above, it is useful to compare the emission intensities of planetary nebulae, HII regions, and T Tauri stars. We will make these comparisons in the context

of the theories for H_2 excitation and we will consider excitation by ultraviolet photons and shock heating to be the two most plausible alternatives. If the H_2 is excited by ultraviolet radiation, objects which show H_2 emission will contain strong ultraviolet luminosity sources, regions of ionized gas, and regions of dense neutral material within or surrounding the regions of ionized gas. If the H_2 is excited behind strong shocks, objects which show H_2 emission will contain strong energy sources or energetic explosions which drive shocks and will be near regions of dense, neutral material.

Both the planetary nebulae and T Tauri stars satisfy all of these criteria. Both types of objects contain sources of ultraviolet radiation and regions of ionized gas. Planetary nebulae certainly contain regions of neutral material as evidenced by the presence of molecular hydrogen. Observations of CO around planetary nebulae and evolved stars (Mufson, Lyon, and Marionni 1975; Lo and Bechis 1976; Zuckerman et al. 1977) indicate that some of these objects contain envelopes of neutral material substantially larger than the regions of ionized gas. Similarly, observations of CO emission (Knapp et al. 1977) and far infrared emission (Harvey, Thronson, and Gatley 1979) show that T Tauri stars are often embedded in regions of relatively dense, neutral gas. Thus, the conditions necessary for the excitation of H_2 by ultraviolet radiation probably exist in many planetary nebulae and T Tauri stars. Furthermore, both types of objects exhibit nebular expansion velocities which could drive shock waves into the surrounding neutral material and excite molecular hydrogen

(Miller 1974 gives a recent review of planetary nebulae; Strom, Strom, and Grasdalen 1975 summarize the properties of T Tauri stars). The molecular hydrogen in these objects could be vibrationally excited by either of the two plausible processes.

HII regions generally do not contain sources to drive strong shock waves and, in this respect, differ from planetary nebulae and T Tauri stars. Although the HII regions will expand as the gas is heated by the absorption of ionizing photons (Spitzer 1968), the expansion velocities tend to be much less than the observed expansion velocities of planetary nebulae and T Tauri stars. We expect that, for shock excitation, the HII regions are less likely to show molecular hydrogen emission than either the planetary nebulae or the T Tauri stars. On the other hand, HII regions contain strong sources of ultraviolet radiation, ionized gas, and are generally surrounded by dense, neutral material (Wynn-Williams and Becklin 1974). The luminosities at 1000 $\mathring{A}$ and the densities of the neutral and ionized regions are essentially the same in HII regions and planetary nebulae. We therefore expect to see molecular hydrogen emission from HII regions almost as frequently as from planetary nebulae and T Tauri stars if the H_2 is excited by ultraviolet radiation.

It can be seen from the table that planetary nebulae often show H_2 emission whereas HII regions do not. Of the nine HII regions in the table, only the area 21" west of θ^2 Ori shows possible H_2 emission. This result is complicated by the fact that a T Tauri star is seen in the same direction. In contrast to this result, we see H_2 emission

from seven of the seventeen planetary nebulae listed in the table. Furthermore, the emission intensities of T Tau, NGC 7027, and CRL 618 are greater than or equal to the upper limits obtained toward almost every HII region. If the H_2 is excited by the absorption of ultraviolet radiation in any object, we might expect to see H_2 emission from some of the HII regions. We conclude that the H_2 excitation in the objects in this sample most probably results from heating behind strong shocks.

The planetary nebulae are particularly appropriate objects to show shock heated H_2 since their expansion velocities often fall within the range of 10 to 25 km s^{-1} required for shock excitation and they typically eject gas with enough energy for the shell ($> 10^{44}$ ergs) to drive a strong shock. If mass loss commonly precedes this ejection in the proto-planetary objects (Lo and Bechis 1976, Zuckerman et al. 1977), then substantial volume densities of H_2 may exist outside of young planetary nebulae. Many of the other objects in the table have some of the characteristics described above but may lack the exact conditions necessary for H_2 emission. The molecular clouds all have relatively large volume densities of molecular hydrogen yet, in all cases, there is no a priori reason to expect strong shock waves in these clouds. The supernova remnant, W 44, is clearly a source of strong shock waves and may be in a region of high density molecular gas seen in CO emission (Wootten 1977) but the shocks in this source could easily be outside of the required velocity range. These examples illustrate the problems encountered when one attempts to interpret the upper limits in the table.

II. H_2 Emission from Orion

Of all known H_2 emission line sources, the highest observed intensity of emission comes from Orion. This intensity, when corrected for extinction, is more than two orders of magnitude greater than that observed from any other object. The intensity and extent of the emission make it several orders of magnitude more luminous than any other observed galactic emission source. These characteristics indicate that a very special set of circumstances probably exist in Orion to cause this emission.

Because of the intensity of the emission from Orion, we can observe many H_2 lines and extend the studies started by Gautier et al. (1976) and Grasdalen and Joyce (1976). Papers 3 and 4 give a reasonably complete picture of the physical conditions within the emission region. This picture results quite naturally from the data and the assumption that the molecules are in thermal equilibrium with their surroundings; particular attention is given to this assumption in the following discussion. A complete summary of the observational results is given below followed by a brief discussion of the implications for the Orion nebula.

a) Geometry

The maps presented in Paper 3 show the direction and extent of the emission region. The emission is roughly centered on the infrared cluster and is approximately 0.2 pc in extent, much smaller than the extent of either the HII region or the molecular cloud. The area over which the emission is seen is thought to be the densest portion of the molecular cloud and within this area many interesting phenomena such as the pres-

ence of high velocity gas seen in CO emission (Zuckerman, Kuiper, and Rodriguez-Kuiper 1976, Kwan and Scoville 1976) and H_2O emission (Genzel and Downes 1977) have been observed.

The extinction measurements of Paper 4 indicate that the emission comes from inside or behind the molecular cloud. The extinction to the molecular hydrogen emission is equal to the extinction inferred to the infrared cluster by Gillett et al. (1975) within the large uncertainties and, because this cluster is generally believed to be inside the cloud, it is likely that the H_2 emission region is also. From the direction, limited extent, and cloud depth of the H_2 emission, we argue that it is associated with the infrared cluster and the core of the molecular cloud.

b) Physical Conditions within the Emission Region

The line intensity measurements of Paper 3, when corrected for extinction, give information about the physical conditions within the region of H_2 emission. By comparing NGC 7027 with Orion and using the reddenning law of van de Hulst (see Paper 4), we derive a 2.1 μm extinction of 4.5 mag to the region of emission in Orion. We have used this extinction with the reddenning law to give the extinction at the wavelength of each H_2 line and our analysis implies the surface brightness and luminosity of the $v = 1 \rightarrow 0$ S(1) line are sixty times greater than the observed values.

The corrected line intensities indicate the hydrogen molecules exist in a region with a kinetic temperature of 2000 K. We have assumed the molecular level populations are in thermodynamic equilibrium with

the kinetic energy states of the gas to obtain this result. There are four arguments for the validity of this assumption. First, the vibrational and rotational temperatures are equal to within the uncertainties. The rotational levels will thermalize at a density at least an order of magnitude smaller than the density necessary for the vibrational levels to thermalize. If the levels were out of thermodynamic equilibrium with the gas, the rotational and vibrational temperatures would probably be different. Second, the H_2 volume densities inferred for the molecular cloud in the direction of the observed H_2 emission (Thaddeus et al. 1971, Liszt et al. 1974, Evans et al. 1975) are large enough to thermalize the rotational levels and are consistent with the densities necessary to bring the vibrational level into equilibrium with the kinetic states of the gas. Third, if shock heating excites the H_2, the densities required to account for the emission intensity are substantially larger than those necessary to thermalize the vibrational levels (see section IIc). As discussed below, shock waves most probably excite the observed molecular hydrogen. Fourth, the line intensity ratios are inconsistent with those predicted by Black and Dalgarno (1976) for pure radiative excitation and subsequent cascades. Thus, even if the molecules are not in strict thermal equilibrium, inelastic collisions probably determine the level populations. Because the rotational and vibrational temperatures agree within the uncertainties, it is likely that the derived temperature of 2000 K is very close to the kinetic temperature of the gas.

Column densities of order 5×10^{20} cm^{-2} have been derived from the data (Papers 3 and 4). This is probably an upper limit; if the volume density of H_2 is too small for thermal equilibrium to obtain, the popula-

tions will cause an underestimate of the temperature and an overestimate of the column density N_o. If the gas is in strict thermal equilibrium, as we have assumed, then N_o is the column density of H_2 at 2000 K.

The observed luminosity of Orion in the $v = 1 \rightarrow 0$ S(1) line is 2.5 $L_\odot$. Assuming a thermal distribution of level populations at 2000 K, we calculate the total luminosity of all the H_2 lines to be about 50 $L_\odot$ and the extinction correction raises this luminosity to 3000 $L_\odot$. Although there is a rather large uncertainty in the extinction, the total power radiated in molecular hydrogen lines alone is certainly of order 1000 $L_\odot$.

If the volume density of H_2 is at least 10^5 cm^{-3} (Thaddeus et al. 1971, Liszt et al. 1974, Evans et al. 1975) and the column density is 5×10^{20} cm^{-2}, the emitting region is of order 10^{-3} pc thick. This thickness is two orders of magnitude smaller than the observed extent of the emission projected on the sky. Thus, the H_2 emission appears to come from a thin sheet of gas, heated to 2000 K, and embedded deep in the cool molecular cloud.

c) Excitation and Energy Source

The results show the emission region to be a hot (T = 2000 K), thin ($< 10^{-3}$ pc) sheet of gas extended over 0.2 pc and buried in the molecular cloud. As shown by Hollenbach and Shull (1977), Kwan (1977), and London, McCray, and Chu (1977), this kind of region is produced quite naturally behind the density discontinuity of a strong shock wave. We will summarize briefly the principal results of the calculations. Kwan was the first author to include the important effects of molecular dissociation; we

refer to his calculation in the following discussion.

As the molecules pass through the shock discontinuity, they suffer elastic collisions which heat the gas to an immediate post-shock temperature T. For fast shocks ($v > 12$ km s^{-1}), T is greater than 5000 K; the molecular dissociation rate above this temperature is large enough to dissociate many of the molecules in the gas. The dissociation rate depends exponentially on the temperature and the rate becomes small below about 5000 K. H_2 dissociations cool the gas until the temperature drops below this value. The gas then cools by emitting radiation in the vibrational lines of molecular hydrogen. These lines dominate all other cooling processes for temperatures above 1000 K; below this temperature, emission in the purely rotational lines of H_2 and CO becomes important. The emission line intensity ratios can be calculated by integrating the collisional and radiative rate equations through the shock front. Kwan's calculation shows that the molecular dissociation acts as a thermostat to keep the effective temperature constant and makes the relative line intensities almost independent of shock velocity v for 10 km s-1 < v < 25 km s^{-1}. The lower limit is established by requiring the shock to have sufficient kinetic energy for the excitation of molecules into the first vibrational state; the upper limit comes about by requiring that the shock not dissociate all of the H_2. The observed line intensity ratios agree with the predicted line intensity ratios within the uncertainties.

The models show, for H_2 volume densities n greater than 10^6 cm^{-3}, the absolute line intensities are almost linearly proportional to n and they are a weak function of shock velocity for $v > 10$ km s^{-1}. The

observations, when used with the models, imply that $n \simeq 3 \times 10^7$ cm^{-3} in Orion. This value is consistent with the value of 10^6 cm^{-3} necessary to establish thermal equilibrium among the vibrational levels, as we have assumed. We note that, for $n < 10^6$ cm^{-3}, the inelastic collisional rates are less than the radiative rates for the vibrational levels (Black, private communication), so the absolute line intensities will be proportional to n^2 and the results of the model calculations cannot be readily extrapolated. At these densities, cooling by purely rotational line emission will become relatively important. The densities we infer for the new H_2 emission sources presented earlier are all of order 10^4 cm^{-3}.

Although we cannot infer the origin of the shock wave in Orion from the observations, we can estimate the amount of energy involved and place useful constraints on the energy source for the shock. An estimate of the lifetime of the shock can be obtained by dividing the radius of the emission region (0.1 pc) by the shock velocity ($\sim$ 20 km s^{-1}); this calculation gives a time of 5000 years. If the H_2 luminosity has been greater than or equal to 1000 $L_\odot$ for the last 1000 years, then at least 10^{47} ergs have been radiated away in H_2 lines. This energy must have been provided by the object or energy source which drives the shock.

The arguments of Hollenbach and Shull (1977), Kwan (1977), and Papers 3 and 4 show no observed energy source in Orion can provide the energy to drive such a shock. Stellar winds from embedded stars, expansion of the HII region, or any process producing a constant pressure to drive the gas fail to provide the necessary energy for the Orion shock. Kwan and Scoville (1976) suggested that a supernova explosion within the molecular cloud would create a shock wave strong enough to excite H_2.

This suggestion is attractive because it explains the presence of high velocity features in CO and H_2O emission. If an explosion caused the Orion shock, then it released at least 10^{47} ergs. This energy could easily come from a supernova (typical energies 10^{49} to 10^{51} ergs) but is substantially larger than that expected from a nova (typically 10^{45} ergs), for example.

Kwan and Scoville based their suggestion on observations of the $\pm$ 60 km s^{-1} gas velocities seen in CO emission. We have lent support to this suggestion by analysing an independent set of observations. It is useful to examine the strengths and weaknesses of the supernova hypothesis in light of all the currently available observational data and several physical arguments.

In support of the suggestion, we make the following observations. First, Kwan and Scoville's arguments indicate that the high velocity gas in Orion most probably comes from a uniformly expanding region. Their arguments show that contraction or rotation cannot plausibly produce the observed line profiles. Second, our analysis of the observations of H_2 emission requires the postulate that some unobserved, energetic source drives a strong shock wave into the dense molecular cloud. Third, in a dense molecular cloud, the initially ionized gas probably recombines soon after the explosion. For example, if we use the total recombination coefficient of hydrogen at a temperature of 10^4 K (Allen 1973) and assume the ionic and electron densities are greater than 10^5 cm^{-3}, we find the recombination time is ten years. We do not necessarily expect a radio remnant from a supernova explosion and the only indication of this event might come from the shocked gas.

Fourth, the Orion nebula is part of a region containing many high mass (O and B type) stars. Orion is possibly just the place where a very high mass star could form, evolve quickly to the supernova stage, and explode while still inside the cloud.

Several recent observations are difficult to reconcile with a simple geometrical model of an explosion. Phillips et al. (1977) show the high velocity CO to be confined to a very small region, less than 15" in radius and centered on the infrared cluster, whereas the H_2 emission is observed to extend almost 90" north of the cluster but is seen along the same line of sight as the CO emission (Paper 3). CO velocities of $\pm$ 60 km s^{-1} are present in the spectra of Kwan and Scoville (1976) and Zuckerman, Kuiper, and Rodriguez-Kuiper (1976). Because a shock with a velocity greater than 25 km s^{-1} will dissociate essentially all the molecular hydrogen which it encounters, we expect the shock wave associated with the H_2 emission ($v < 25$ km s^{-1}) to precede the 60 km s^{-1} gas. These observations imply that the H_2 emission originates in an extended, slow moving shock front outside of a compact, rapidly expanding region from which the CO emission arises. In a simple explosion, however, the highest velocity gas precedes the gas with lower velocities. Kwan (1977) argues that the gas flow must be anisotropic to resolve this problem. The CO emission profile of Zuckerman, Kuiper, and Rodriguez-Kuiper is very symmetric and there is no indication of any anisotropy in the gas flow. Finally, Joyce et al. (1978) observe the H_2 emission line profile to be less than 30 km s^{-1} wide (unresolved) and centered on the rest velocity of the molecular cloud. They interpret their results by assuming the emission comes from an expanding shell with the front and back sides

contributing equally. In view of the large cloud densities we have derived, we would expect a substantial amount of extinction due to dust between the two sides of the shell, thus, completely obscuring emission from the back side. Barlow and Silk (1977) show that dust grains are destroyed by sputtering in strong shocks. They conclude, however, that shock velocities greater than 100 km s^{-1} are needed to destroy most grains and shock velocities greater than 200 km s^{-1} are needed to destroy silicate core grains. Silicate grains are observed in the Orion region by Gillett et al. (1975). Hall et al. (1978) observe a component in the 5 μm CO absorption profiles that is blue shifted by about 25 km s^{-1} with respect to the rest velocity of the cloud and this component quite possible originates in the region of shocked gas associated with the H_2 emission. If so, Joyce et al. may have observed a component of the shock which is moving perpendicular to the line of sight.

The observed size of the shocked region and theoretical lower limit to the shock velocity imply that the explosion must have occurred only a few thousand years ago. The short lifetime of the shock makes it rather unlikely that we would observe this event. On the other hand, the observations of strong H_2 emission and high velocity CO emission are unique to Orion at this time. It is perhaps just the transient nature of this event which makes it improbable that we will observe these phenomena anywhere else in the galaxy.

III. Concluding Remarks

We conclude by summarizing the important results obtained from the analysis of H_2 emission sources and by briefly discussing the need for

further study. The number of objects which show H_2 emission, while small, is encouraging since the observed line intensities in most of the new sources are near the current detection limit. As our techniques improve, H_2 emission may be commonly detected in celestial objects, so we must understand the useful implications of such detections for these objects. The observations and analysis presented in this thesis lead to a consistent interpretation of the implications for several sources of H_2 emission. They have enhanced our understanding of the nature of H_2 emission from all such sources.

We have restricted our attention to the detailed nature of H_2 emission and, in so doing, we have neglected the discussion of many important questions raised by this work. Many of these questions arise from the implication that relatively high density molecular regions must exist in all of the objects which show H_2 emission. It is not yet known how these regions form, how the molecules are protected from the harsh environments present in most of the objects, how the regions evolve, and what these regions may tell us about the objects themselves. These questions will be left for future studies. Additionally, substantial progress on the understanding of interstellar H_2 must still be made. This work adds only a small amount to the overall understanding of H_2 excitation. A number of unavoidable uncertainties remain in the study; it is important to verify our main conclusions.

Listed below are several suggestions for future observational and theoretical work stimulated by the results of this thesis:

1. The conclusion that shock excitation is the most important source of H_2 emission must be verified. A measurement of the $v = 2 \rightarrow 1$ S(1)

line from any of the new sources provides a discriminant between the shock theory and the ultraviolet pumping theory. Additionally, the discovery of H_2 emission from an object containing no source of ultraviolet radiation would lend support to this conclusion.

2. New sources of H_2 emission will enlarge the already growing sample and allow statistical analyses of source properties. The search for new sources is aided by the observation that high hydrodgen densities and gas velocities between 10 and 25 km s^{-1} are necessary for H_2 emission.

3. From the detection of H_2 emission in a celestial object, we can infer a number of physical parameters in that object. For example, if the H_2 emission region can be spatially resolved, and if measurements of the line velocity and intensity of the $v = 2 \rightarrow 1$ S(1) line can be made, we can immediately calculate the temperature, density, and luminosity of the emission region. Furthermore, we can infer the energy of the shock as we have in Orion. This information may place important contraints on such quantities as the energy released during the formation of a planetary nebula. The density of H_2 may, similarly, allow us to calculate the mass of neutral material around objects such as planetary nebulae using a simple model for the density distribution. A detailed analysis of the effects of the strong ultraviolet radiation from planetaries on the surrounding molecular envelopes may tell us the structure of the envelopes or indicate that the molecules are protected inside dense neutral condensations.

4. The rotational lines of H_2 may be measured in many of the new sources. These measurements, while giving information about the H_2 emission, will allow us to refine the observational techniques and interpretation of the measurements and, eventually, make possible widespread observations of molecular hydrogen.

5. Further observations of Orion are very important and could determine the nature of the source which powers the shock. Observations of the high velocity CO with good spatial resolution should be made with the first millimeter wavelength interferometers to sort out the geometrical problems discussed in section IIc. A measurement of the H_2 line profiles with good (several km s^{-1}) spectral resolution is needed to identify the shock velocity and resolve the uncertainties in the Joyce et al. (1978) experiment. A good theoretical model of a supernova explosion within a dense molecular cloud ($n \simeq 10^7$ cm^{-3}) could predict specific observational tests of the supernova hypothesis.

REFERENCES

Aannestad, P. A. 1973, Ap. J. Suppl., 25, 205.

Allen, C. W. 1973, Astrophysical Quantities, p. 95, The Athlone Press University of London, London.

Barlow, M. J. and Silk, J. 1977, Ap. J. (Letters), 211, L83.

Black, J. H. 1978, Ap. J., 222, 125.

Black, J. H. and Dalgarno, A. 1976, Ap. J., 203, 132.

Cahn, J. H. and Kaler, J. B. 1971, Ap. J. Suppl., 22, 319.

Evans, N. J., II, Zuckerman, B., Sato, T., and Morris, G. 1975, Ap. J., 199, 383.

Field, G. B., Rather, J. D. G., Aanestad, P. A., and Orszag, S. A. 1968, Ap. J., 151, 953.

Gautier, T. N., III, Fink, U., Treffers, R. R., and Larson, H. P. 1976, Ap. J. (Letters), 207, L129.

Genzel, R. and Downes, D. 1977, Astr. Ap., 61, 117.

Gillett, F. C., Forrest, W. J., Merrill, K. M., Capps, R. W., and Soifer, B. T. 1975, Ap. J., 200, 609.

Gould, R. J. and Harwit, M. 1963, Ap. J., 137, 694.

Grasdalen, G. L. and Joyce, R. R. 1976, B.A.A.S., 8, 349.

Hall, D. N. B., Kleinman, S. G., Ridgway, S. T., and Gillett, F. C. 1978, preprint.

Harvey, P. M., Thronson, H. A., and Gatley, I. 1979, in preparation.

Hollenbach, D. and Salpeter, E. E. 1971, Ap. J., 163, 155.

Hollenbach, D. J. and Shull, J. M. 1977, Ap. J., 216, 419.

Hollenbach, D. J., Werner, M. W., and Salpeter, E. E. 1971, Ap. J., 163, 165.

Joyce, R. R., Gezari, D. Y., Scoville, N. Z., and Furenlid, I. 1978, Ap. J. (Letters), 219, L29.

Knapp, G. R., Kuiper, T. B. H., Knapp, S. L., and Brown, R. L. 1977, Ap. J., 214, 78.

Kwan, J. 1977, Ap. J., 216, 713.

Kwan, J., and Scoville, N. 1976, Ap. J. (Letters), 210, L39.

Liszt, H. S., Wilson, R. W., Penzias, A. A., Jefferts, K. B., Wannier, P. G., and Solomon, P. M. 1974, Ap. J., 190, 557.

Lo, K. Y. and Bechis, K. P. 1976, Ap. J. (Letters), 205, L21.

London, R., McCray, R., and Chu, S. I. 1977, Ap. J., 217, 442.

Miller, J. S. 1974, Ann. Rev. Astron. Ap., 12, 331.

Mufson, S. L., Lyon, J., and Marionni, P. A. 1975, Ap. J. (Letters), 201, L85.

Phillips, T. G., Huggins, P. J., Neugebauer, G., and Werner, M. W. 1977, Ap. J. (Letters), 217, L161.

Shull, J. M. 1978, preprint.

Spitzer, L., Jr. 1968, Diffuse Matter in Space, p. 183, Interscience Publishers, New York, New York.

Spitzer, L., Jr. and Cochran, W. D. 1973, Ap. J. (Letters), 186, L23.

Strom, S. E., Strom, K. M., and Grasdalen, G. L. 1975, Ann. Rev. Astron. Ap., 13, 187.

Thaddeus, P., Wilson, R. W., Kutner, M., Penzias, A. A., and Jefferts, K. B. 1971, Ap. J. (Letters), 168, L59.

Treffers, R. R., Fink, V., Larson, H. P., and Gautier, T. N., III. 1976, Ap. J., 209, 793.

Willner, S. P. 1976, Ap. J., 206, 728.

Wootten, H. A. 1977, Ap. J., 216, 440.

Wynn-Williams, C. G. and Becklin, E. E. 1974, Publ. A. S. P., 86, 5.

Zuckerman, B., Kuiper, T. B. H., and Rodriguez-Kuiper, E. N. 1976, Ap. J. (Letters), 209, L137.

Zuckerman, B., Palmer, P., Morris, M., Turner, B. E., Gilra, D. P., Bowers, P. F., and Gilmore, W. 1977, Ap. J. (Letters), 211, L97.